

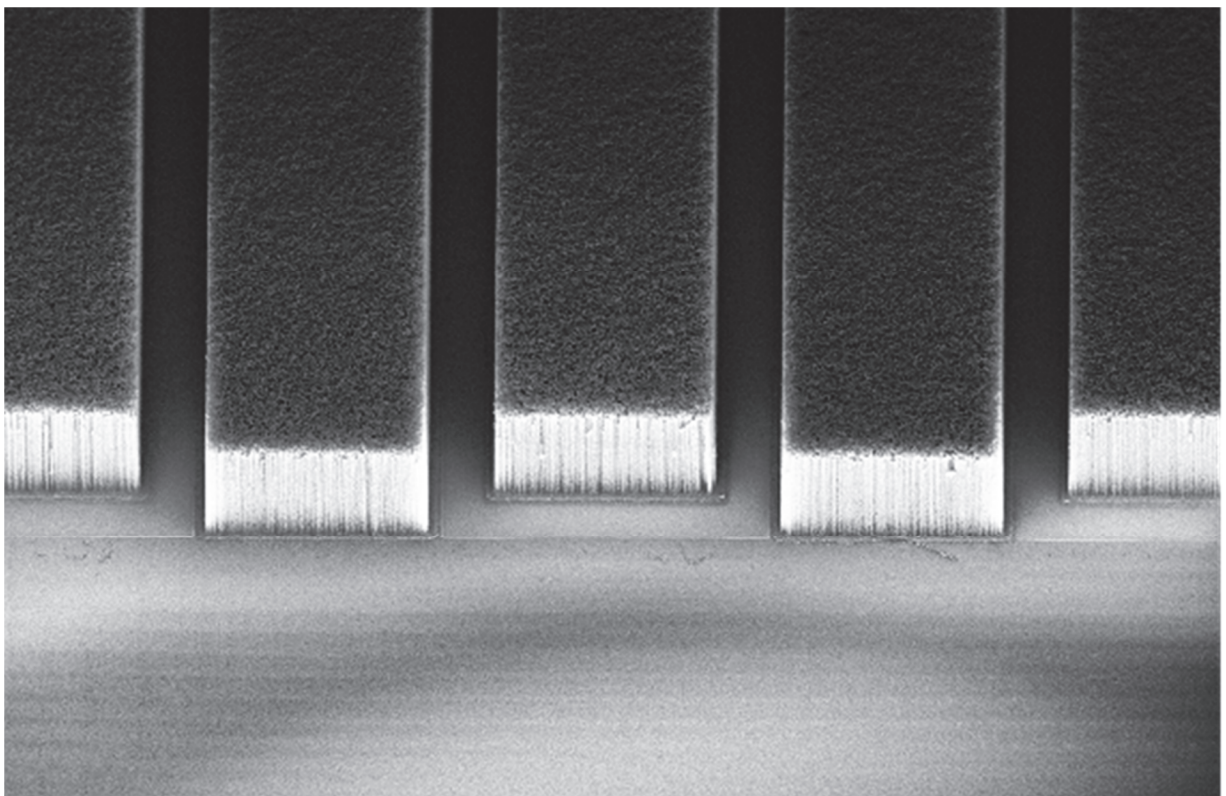


Final public report, date: 04.07.2023

---

# **SWift energy charging Super-capaciTOR based on carbon nanotube arrays**

---



Source: ©EPFL 2022



**EPFL**

**Date:** 19.03.2023

**Location:** Bern

**Publisher:**

Swiss Federal Office of Energy SFOE  
Energy Research and Cleantech  
CH-3003 Bern  
[www.bfe.admin.ch](http://www.bfe.admin.ch)

**Co-financing:**

EPFL, Nanolab  
Route Cantonale, CH-1015, Lausanne  
<https://www.epfl.ch/labs/nanolab/>  
<https://www.epfl.ch>

**Subsidy recipients:**

EPFL, Nanolab  
Route Cantonale, CH-1015 Lausanne  
[www.epfl.ch](http://www.epfl.ch)

**Authors:**

Hung-Wei Li, EPFL, [hung-wei.li@epfl.ch](mailto:hung-wei.li@epfl.ch)  
Adrian Ionescu, EPFL, [adrian.ionescu@epfl.ch](mailto:adrian.ionescu@epfl.ch)  
Victoria Manzi, EPFL, [victoria.manzi@epfl.ch](mailto:victoria.manzi@epfl.ch)  
Clara Moldovan, EPFL, [clara.moldovan@epfl.ch](mailto:clara.moldovan@epfl.ch)  
Justyna Piwek, EPFL, [justyna.piwek@epfl.ch](mailto:justyna.piwek@epfl.ch)

**SFOE project coordinators:**

Men Wirz, [Men.Wirz@bfe.admin.ch](mailto:Men.Wirz@bfe.admin.ch)  
Roland Brueniger, [roland.brueniger@brueniger.swiss](mailto:roland.brueniger@brueniger.swiss)

**SFOE contract number:** SI/502151-01

**The authors bear the entire responsibility for the content of this report and for the conclusions drawn therefrom.**



## Zusammenfassung

Heutige Lithium-Ionen-Batterien sind mit mehreren Einschränkungen konfrontiert: langsames Aufladen, begrenzte Lebensdauer und Sicherheitsprobleme, mit zusätzlichen negativen sozialen und ökologischen Auswirkungen aufgrund ihres Lithium- und Kobaltbedarfs. Ziel dieses Projekts ist die Entwicklung einer neuartigen Energiespeicherlösung als Ersatz für wiederaufladbare Batterien, die auf einem Superkondensator aus Kohlenstoffnanoröhren (CNT) basiert. Im Gegensatz zu einer Lithium-Ionen-Batterie ist die vorgeschlagene Technologie umweltfreundlich, lässt sich schnell aufladen (10- bis 100-mal schneller als herkömmliche Batterien), hat eine längere Lebensdauer (> 20'000 Zyklen) und kann ohne Sicherheitsprobleme in einem breiten Temperaturbereich betrieben werden. Darüber hinaus kann ein Superkondensator aufgrund der großen Oberfläche der CNT in Verbindung mit einem intelligenten Gerätedesign und einer Nanostrukturierung, hohe Energieniveaus speichern, mit allen zusätzlichen Vorteilen von Superkondensatoren, und er hat auch einen geringen Zugangswiderstand dank des Wachstums der CNT auf leitfähigen Substraten und einem originellen Elektrodendesign. Zusätzlich zu den technischen Leistungen, die über den Stand der Technik hinausgehen, kann die vorgeschlagene Technologie mit Hilfe von Reinraum-Fertigungstechniken skaliert werden und ist in der Lage, sowohl die Anforderungen von IoT-Knoten als auch von tragbaren Geräten zu erfüllen, mit nachgewiesenem kommerziellen Wert und großen wirtschaftlichen Auswirkungen.

Die wichtigsten bisher erzielten Ergebnisse sind die Entwicklung von Superkondensatoren auf der Basis von dichten, vertikal ausgerichteten CNTs (VACNTs) mit Dichten von bis zu  $0,85 \times 10^{12}$  CNT/cm<sup>2</sup> auf Metallelektroden, die sich ideal für miniaturisierte Energiespeicherung auf Chips eignen. Im Rahmen dieses Projekts wurden Bauelementdesigns mit maximaler aktiver Fläche und eine skalierbare Herstellung für die Integration in elektronische Systeme optimiert. Wir untersuchten und optimierten verschiedene pseudokapazitive Schichten aus nanometrischen Metalloxiden für eine verbesserte Energiedichte. Die wichtigste Errungenschaft dieses Projekts ist die ganzheitliche Entwicklung von miniaturisierten hybriden Superkondensatoren mit einem weniger toxischen ionischen Elektrolyten, der eine Leistungssteigerung ermöglicht. Die CNT (mit Bundles)/MnO<sub>2</sub>-Hybridmaterialien weisen eine hohe spezifische Kapazität und eine gute Zyklenstabilität auf. Die CNTs verbessern die elektronische Leitfähigkeit der Hybridmaterialien, was zu einem geringeren Innenwiderstand der Superkondensatoren führt. Wir erzielten eine bis zu 2-fache Verbesserung der spezifischen Kapazität auf bis zu 90 mF.cm<sup>-2</sup> und einen Widerstand von unter 30 Ω, der mit den VACNT-basierten Elektroden erheblich optimiert werden kann. Außerdem haben wir erfolgreich ionische Flüssigelektrolyte mit einem Spannungsfenster von 2,5 V integriert. Dieses Projekt stellte auch eine Machbarkeitsstudie von Superkondensatoren für IoT-Knoten dar und definierte die Anforderungen und das Potenzial der Technologie für Sensoranwendungen. Es war ein wesentlicher Meilenstein für miniaturisierte Superkondensatoren, die in elektronische Systeme integriert sind, und ermöglichte uns aus geschäftlicher Sicht, unsere Strategie für die Markteinführung zu entwickeln.

## Résumé

Les batteries Li-ion actuelles ont une série de limitations, comme la charge lente, la durée de vie limitée et des problèmes de sécurité. De plus leur technologie est basée sur l'utilisation des matériaux rares comme le Li et le Co, ce qui peut induire des limitations environnementales et sociales. Le but de ce projet est de développer une nouvelle solution de stockage d'énergie basée sur des supercondensateurs à base de nanotubes de carbone (CNTs). Cette solution est écologique et a des performances uniques, comme une excellente vitesse de recharge (10 à 100 fois plus rapide qu'une batterie traditionnelle), une durée de vie accrue (>20'000 cycles) et une large gamme d'utilisation sans de problèmes de sécurité. La solution technologique adoptée offre l'avantage d'une grande surface d'électrode en exploitant des réseaux de nanotubes de carbone, qui en plus sont très stables chimiquement. Ceci offre la possibilité de stocker une grande densité d'énergie avec des résistances



d'accès réduites. La technologie est basée sur la croissance des CNTs sur des substrats conducteurs et exploite un design original de l'électrode. Cette technologie est facilement scalable en production car elle utilise des procédés de salle blanche et est capable de répondre aux besoins des applications IoT et téléphone intelligents, avec une grande valeur commerciale ajoutée et grand potentiel économique.

Les principaux résultats obtenus à ce jour sont le développement de supercondensateurs à base de CNT denses alignés verticalement (VACNT) avec des densités allant jusqu'à  $0,85 \times 10^{12}$  CNT/cm<sup>2</sup> sur des électrodes métalliques, idéaux pour le stockage d'énergie miniaturisé sur puce. Ce projet a optimisé les conceptions de dispositifs à zone active maximisée et une intégration aux systèmes électroniques. Nous avons étudié et optimisé diverses couches pseudocapacitives d'oxydes métalliques nanométriques pour obtenir une meilleure densité d'énergie. La principale réalisation de ce projet est le développement holistique de supercondensateurs hybrides miniaturisés avec un électrolyte ionique moins toxique, offrant un gain de performances. Les matériaux hybrides CNT (avec bundles)/MnO<sub>2</sub> ont montré une capacité spécifique élevée et une bonne stabilité au cyclage. Les CNT améliorent la conductivité électronique des matériaux hybrides, ce qui se traduit par une plus faible résistance interne des supercondensateurs. Nous avons obtenu une amélioration de la capacité spécifique jusqu'à 2 fois, jusqu'à 90 mF.cm<sup>-2</sup> et une résistance inférieure à 30 Ω, qui peut être considérablement optimisée avec les électrodes à base de VACNT. De plus, nous avons intégré avec succès des électrolytes liquides ioniques avec une tension de 2,5 V. Ce projet a également constitué une étude de faisabilité de supercondensateurs pour les nœuds IoT, définissant les exigences et le potentiel de la technologie pour les applications de capteurs et a été un tremplin essentiel pour les supercondensateurs miniaturisés intégrés aux systèmes électroniques ainsi que d'un point de vue commercial permettant à préparer les prochaines étapes de développement d'une stratégie de mise sur le marché.

## Summary

Today's Li-ion rechargeable batteries are facing several limitations: slow charging, limited lifetime and safety issues, with additional social and environmental negative implications due to their need of lithium and cobalt. This project aims at developing a novel energy storage solution to replace rechargeable batteries, based on a carbon nanotube (CNT) supercapacitor. In contrast with a Li-ion battery, the proposed technology is ecologically friendly, exhibits fast charging (10 to 100 times faster than traditional batteries), extended lifetime (> 20'000 cycles) and a wide range of operating temperatures without security issues. Moreover, due to the CNT high surface area combined with a smart device design and nanostructuring, a supercapacitor could store very high energy levels, with all the added advantages of supercapacitors, and it also has low access resistance thanks to growth of CNTs on conductive substrates and to an original electrode design. In addition to the technical performances that are beyond the state of the art, the proposed technology can be scaled-up using clean room fabrication techniques, being capable to address both demands of IoT nodes and of hand-held devices, with demonstrated commercial value and large economic impact.

The main results achieved up to date are the development of supercapacitors based on dense vertically aligned CNTs (VACNTs) with densities up to  $0.85 \times 10^{12}$  CNT/cm<sup>2</sup> on metallic electrodes, ideal for miniaturized energy storage on-chip. This project optimized maximized active area device designs and a scalable fabrication to be integrated with electronic systems. We studied and optimized various pseudocapacitive layers of nanometric metal oxides for improved energy density. The main achievement of this project is the holistic development of miniaturized hybrid supercapacitors with a less toxic ionic electrolyte, offering a boost in performance. The CNT(with bundles)/MnO<sub>2</sub> hybrid materials showed a high specific capacitance and good cycling stability. The CNTs improve the electronic conductivity of the hybrid materials, which resulted in a lower internal resistance of the supercapacitors. We obtained an improvement in specific capacitance up to 2-fold, up to 90 mF.cm<sup>-2</sup> and a resistance below 30 Ω, which can be significantly optimized with the VACNT based electrodes. Moreover, we have successfully integrated ionic liquid electrolytes with a 2.5 V voltage window. This project also constituted a feasibility study of supercapacitors for IoT nodes, defining the requirements and potential of the technology for





sensor applications and was an essential steppingstone for miniaturized supercapacitors integrated with electronic systems as well as from a business perspective, allowing us to develop our go to market strategy.

## Main findings

- Randomly aligned CNTs, mixed with metal oxides were benchmarked with the VACNTs coated with metal oxides and they yielded superior performance in terms of areal capacitance and comparable in terms of gravimetric capacitance. This electrode materials are limited to ink printing feature size for on-chip processing (in the order of 100  $\mu\text{m}$  feature size mean while for VACNT feature below 10  $\mu\text{m}$  are achivable). But they could be cheaper than VACNT and scalable for some electrochemical capacitors.
- Ionic liquids are promising electrolytes for mesoporous supercapacitor electrodes due to the compatibility of ion size with the porosity of the electrode and a voltage window of 3.5 V can be achieved in double layer supercapacitors for high power applications and 2.4 V in metal oxide enhanced supercapacitors for applications requiring higher energy.
- The long-term cycling experiments show that for devices based on Vertically aligned CNTs (VACNTs) coated with electrochemically deposited metal oxides the system is stable up to 20'000 cycles, which is larger than SOA. The loss of performance criteria are a 20 % initial capacitance fade or a resistance increase layer than 50%. This was demonstrated for very small loadings as a proof of concept and further work is required for device optimization and understand the physical dependencies. Until now, the experiments with CNT bundles and  $\text{MnO}_2$  reached 5'000 cycles without any problem; the expectation is that the continuation of the experiments will demonstrate stability up to a much higher number of cycles.
- We screened and identified the optimal electrolytes for metal oxide enhanced supercapacitors. Ionic liquid based electrolytes are very promising electrolytes for CNT/Metal oxides based supercapacitors, yielding extended lifetime compared to the state-of-the-art.



# Contents

Zusammenfassung .....	3
Résumé .....	3
Summary .....	4
Main findings .....	5
Contents .....	6
Abbreviations .....	7
1 Introduction .....	8
1.1 Background information and current situation .....	8
1.2 Purpose of the project .....	9
1.3 Objectives .....	10
2 Procedures and methodology .....	10
2.1 Fabricated Prototypes and Tested Devices .....	11
2.2 Nanocarbon Electrodes Fabrication .....	13
2.3 On-chip capacitors design optimization .....	13
2.4 Pseudocapacitive layer integration .....	13
2.5 Electrochemical characterization .....	14
3 Results and discussion .....	16
3.1 Decorated CNT electrodes and alternative electrodes .....	16
3.2 Thin film .....	19
3.3 Electrode characterization .....	22
3.4 Integration of Pseudocapacitive layer .....	24
3.5 Electrolyte development .....	26
3.6 Supercapacitor demonstrator and tests of figures of merit .....	30
3.7 Fabrication Scaling and Cost Assessment .....	35
3.8 Dissemination and Communication .....	36
3.9 Interaction with the Industrial Advisory Board .....	36
4 Conclusions .....	37
5 Outlook and next steps .....	38
6 National and international cooperation .....	38
7 Publications .....	39
8 References .....	39
9. Appendix .....	42



## Abbreviations

AFM: Atomic Force Microscope

ALD: Atomic Layer Deposition

BMIM BF<sub>4</sub>: 1-butyl-3-methylimidazolium tetrafluoroborate

BRNC: Binning and Rohrer Nanotechnology Center

CIME: Interdisciplinary Centre for Electron Microscopy

CNT: Carbon Nanotubes

CV: Cyclic Voltammetry

CVD: chemical vapor deposition

EDNA: Electronic Devices & Network Annex

EDX: Energy-dispersive X-ray Spectroscopy

EIS: Electrochemical Impedance Spectroscopy

EMIM BF<sub>4</sub>: 1-ethyl-3-methylimidazolium tetrafluoroborate

EPFL: École polytechnique fédérale de Lausanne

GCD: galvanostatic charge/discharge

IBM: International Business Machines Cooperation

IMT: National Institute for Research and Development in Microtechnologies

IoT: internet of things

IR: Ohmic drop, voltage drop

ISIC: Institute of Chemical Sciences and Engineering

LIMNO: Laboratory for Molecular Engineering of Optoelectronic Nanomaterials

LPI: Laboratory of Photonics and Interfaces

PEDOT:PSS: Poly(3,4-ethylenedioxythiophene)-poly(styrenesulfonate)

PVA: poly(vinyl alcohol)

RT: room temperature

SEM: scanning electrochemical microscopy

SC: Supercapacitor

SWCNT: Single Walled carbon nanotube

VACNT: Vertically Aligned Carbon Nanotubes

WP: workpackage

WSN: Wireless Sensor Network

XPS: X-Ray photoelectron Spectroscopy

XRD: X-ray Diffraction



# 1 Introduction

## 1.1 Background information and current situation

While smartphones, smart homes and smart wearables are advancing every year, their larger take-up and impact are limited by power consumption, energy storage being the main bottleneck for IoT larger deployment today. Technology and car companies are all affected by the limitations of current battery technologies. There is a clear market need of improved energy solutions for portable electronics, electric vehicles, storage of energy generated by alternative solutions, autonomous IoT nodes, etc., as current solutions have reached fundamental limitations in terms of energy density, they charge slowly, degrade after 500 -1'000 charging cycles, they are affected by extreme temperatures (with risks of leakage and/or even explosion) and use toxic and dangerous materials.

The IoT market is rapidly emerging and expected to reach \$5 billion by 2025. The Electronic Devices & Network Annex (EDNA) report on Energy Efficiency of the Internet of Things forecasts that more than 23 billion batteries powered IoT devices in 2025. It is also emphasized that users of IoT devices would require a battery that lasts for more than 5 years and current battery technologies have severe limitations for this use case, they have a reduced lifetime and changing them yields high maintenance costs, they get degraded at low or high temperatures, limiting their use, pose safety issues and more importantly this has a huge negative impact on the environment throughout all the value chain, from metals mining to battery manufacturing.

Miniaturized sensor nodes are widely investigated to be implemented within a Wireless Sensor Network (WSN) for the internet of things (IoT) and powering these nodes is still challenging due to the miniaturization of such devices. Energy harvesting technologies have attracted a great deal of attention for IoT devices and self-powering systems, using mechanical, thermal or solar energy. The instability of such resources imposes the use of energy storage technologies compatible with the desired application. In this regard, electrochemical capacitor, also known as supercapacitors (SCs) have gained a lot of attentions due to their unique properties like high power density, long cycle life and environment friendly nature. They act as a link for energy-power difference between a traditional capacitor (high power) and batteries (high energy) [1]–[4].

Supercapacitors are emerging energy storage devices with great potential to supplement batteries, addressing the weakest points of battery technology such as low power, limited number of cycles and low performance at low or too high temperatures or store energy in specific applications requiring fast charging and extended lifetime. The main limitation to their use being the low energy density, self-discharge and high costs. This project focuses on boosting energy density, the main bottle neck for the industrial adoption of supercapacitor technologies.

Porous carbon is the main investigated electrode material used in electrochemical micro-supercapacitors due to its high stability [4]–[7]. High capacitance values up to 1410 mF/cm<sup>2</sup> with a power density of 246.9 mW/cm<sup>3</sup> have been reported using activated carbon [8]. Carbon nanotubes (CNTs) have been widely studied since their discovery in 1991 [9] and attracted extensive attention due to their intriguing and potentially useful structural, electrical and mechanical properties. CNTs have a novel structure, a narrow distribution of size in the nanometer range, highly accessible surface area, low resistivity, and high stability. These features make CNTs suitable for polarizable electrodes and hence, electrochemical supercapacitor component. Supercapacitors with values as high as 1300 mF/cm<sup>2</sup> (energy density of 1.3 mWh/cm<sup>2</sup> and power density of 46 mW/cm<sup>2</sup>) have been reported[10]–[14]. On the other hand, composites incorporating a nanotubular backbone coated by an active phase with pseudocapacitive properties, such as CNT/oxide composite, represent an important breakthrough for developing a new generation supercapacitors based on three basic reasons [15], [16]: (1) the percolation of the active particles is more efficient with nanotubes than with the traditional carbon materials; (2) the open mesoporous network formed by the entanglement of nanotubes allows the ions



to diffuse easily to the active surface of the composite components; and (3) since the nanotubular materials are characterized by a high resiliency, the composite electrodes can easily adapt to the volumetric changes during charge and discharge, which improves drastically the cycling performance. Several pseudo materials such as  $\text{MnO}_2$ ,  $\text{RuO}_2$ ,  $\text{Cu}_x\text{O}$  and MXene [17]–[19] have been investigated during past decade to improve the performance of supercapacitors. It has been shown that the deposition of  $\text{MnO}_2$  on PEDOT:PSS can provide a high capacitance value of  $1670 \text{ mF/cm}^2$  with an outstanding cycling stability of 99.5% after 4'000 cycles [20]. Another critical parameter of supercapacitors is the operating voltage (or voltage window) which highly depends on the electrolyte property. The electrolyte options can be mainly categorized as aqueous, organic, ionic liquid and gels. Aqueous-based electrolytes have been extensively used in SCs [21]–[23] and are able to support a voltage window in the range of 0.8 V to 1.6 V. On the other hand, ionic liquids and organic media are capable of operating with a voltage operation range of up to 3 V [24]–[26].

Despite the fact that encouraging results have been attained in this field, the evolution of new generation of SCs is still at a premature stage. The performance of current supercapacitors is still behind commercial batteries and a low-cost industrial manufacturing process is required for the next generation of SCs. In this regard, this project will be focusing on the following aspects to improve supercapacitor technology and find a route for the realization of the next generation of environmentally friendly energy storage systems:

- Electrode: Developing a reliable fabrication process for CNTs.
- Pseudo capacitive layer: investigating  $\text{MnO}_2$  and developing a synthesis process.
- Enhancing the energy density that is still below of the needs of many applications.
- Enhancing operational voltage window: The selection and optimization of the electrolyte for the SCs are fundamentally necessary to improve the energy storing capacity. The majority of research on the SCs is conducted on electrode materials. However, the electrolyte is equally responsible for the resultant electrochemical performance. Typically, both electrode materials and the electrolyte can affect the resultant cell voltage. Therefore, it is essential to develop the electrolyte having high ionic conductivity, good thermal stability, and high voltage window stability.

## 1.2 Purpose of the project

The innovative principle proposed in this project is based on hybrid SC using highly conductive CNTs and a device design architecture minimizing the resistance and the ionic distance, thus increasing specific capacitance and performance of miniaturized SC device, combined with an optimized additional pseudo-capacitance using nanoscopic coatings in order to push the current values of the state of the art. In addition, we aim to optimize the electrolyte to achieve high ionic conductivity, large electrochemical window, no depletion problems and a high temperature stability, while using environmentally friendly and abundant materials. This allows us to achieve an energy density superior to the state of the art using scalable methods and environmentally friendly materials.

The proposed architecture on CNT arrays allows on-chip integration, which is opening new system-level power management design advances for miniaturized autonomous IoT sensing nodes [6], where the energy storage element lifetime and charging time are key performance parameters leading to a cost effective, maintenance free, continuous power source.

We aim to address needs in the energy storage market by introducing a solution that enables the use of novel autonomous technologies, has a reduced environmental impact, and creates social and economic value. The properties of the proposed energy storage device will contribute to the market acceptance of a new technology in a very competitive environment and will constitute an important stepping-stone to the adoption of a green and efficient battery replacement.





## 1.3 Objectives

We aim to optimize our scalable fabrication processes to match the industrial requirements and standards. This will allow us to obtain a complete competitive energy storage solution and establish the specifications for our product and test it with potential customers.

This project has two main objectives:

- To optimize our scalable fabrication processes to match the industrial requirements and standards. This will allow us to obtain a complete competitive energy storage solution and establish the specifications for our product and test it with potential customers.
- On the business side, we aim to establish strategic partnerships with industrialization partners and potential customers. Based on customer feedback on our technology we aim to refine our market entry strategy and identify the best candidates to establish pilot projects for product industrialization and at the appropriate insertion points in the industrial value chain.

By exploiting nanotechnology, novel materials and optimizing the device design, we obtain a cutting-edge technology enabling a new generation of storage devices which will change the way we charge our mobile devices and electric vehicles.

Specific Objectives defined in the project:

- A. Complete energy storage solution.
  1. High density aligned electrodes with low contact resistance
    - I. Substrate and catalyst optimization and control for a scalable industrial process.
    - II. CNT Growth process optimization resulting in low contact resistance (in the order of 10  $\Omega$ ).
  2. Optimize industrial deposition process developed for the pseudo-capacitive materials on the electrodes in order to have an optimum layer which will significantly boost device performance. Test the decorated CNT hybrid supercapacitors in the field, validating their efficiency and lifetime for the specified use case.
  3. Fabricate complete energy storage solution: with high voltage window, large operative temperature stability -20 to 80 °C. Integrate electrolytes which are environmentally friendly and simplify the fabrication and packaging, essentially decreasing costs, in a scalable process.
  4. Feasibility study of on-chip integration and possibility to integrate it in standard semiconductor processes, directly on the device chip, which will significantly reduce costs, size and the overall system consumption. Metrics: price, market response, ease of integration with the systems of our customers.
  5. Demonstrate energy storage solution in a field test of self-powered IoT nodes: Capacitance 1 mF/cm<sup>2</sup>, Resistance < 10 Ohm, Energy > 100 Wh/kg, lifetime > 30'000 cycles.
- B. Benchmark results with state of the art and with competitor solutions, identify the most important players on the targeted market, adapt market entry strategy and identify strategic partnerships.

## 2 Procedures and methodology

The development of the miniaturized electrochemical capacitor was accomplished based on dedicated work packages (WP).

WP1 focused on the development and optimization of the different needed elements: the CNT electrodes as vertically aligned carbon nanotubes (VACNT) or CNT bundles, metal oxide deposition and electrolyte compatibility. The materials were developed considering scalable methods and environmentally friendly materials.



In WP2 the main target is to integrate and test the full performance of developed devices, with the aim to obtain a micro capacitor with large voltage window, extended temperature stability and long-lasting lifetime. With high energy density and specific capacitance.

## 2.1 Overview of devices and prototypes

Here we present the used tested devices, their components and the overall description of the capacitors employed in this project.

The main tool used on the material development phase is a standard assembly SC configuration (Figure 1). The Swagelok cells allows for standardized and repeatable material testing allowing fast and adaptable SC cells for material screening and optimization, especially when testing metal oxide incorporation and electrolytes compatibilities.

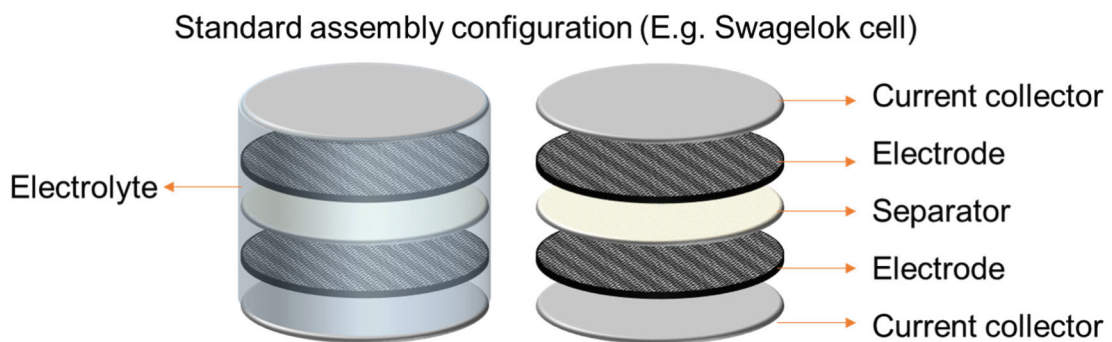


**Figure 1** Sketch representing standard electrochemical capacitor cell configuration.

We also worked on developing and optimizing VACNT on-chip. For this kind of tests, we employed single electrode chips to characterize the electrode material and electrolyte-substrate compatibilities and simple micro capacitor on-chip as a proof of concept. Sketches and pictures are presented in Figure 2 and Figure 3.

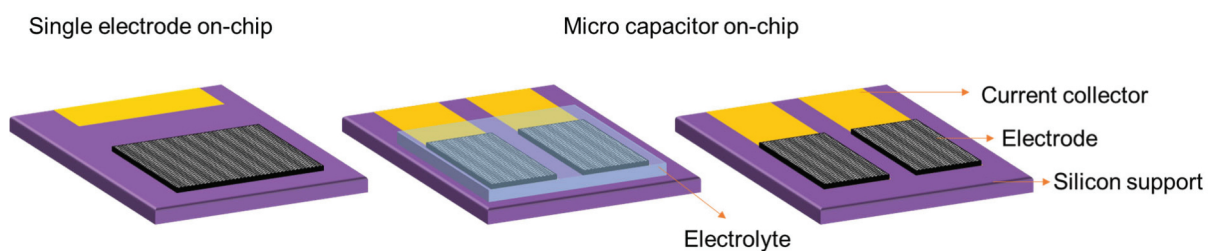


**Figure 2** Sketch of on-chip single electrodes and full cell devices.

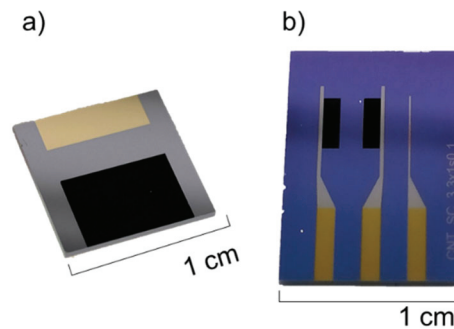


**Figure 3** Images of the on-chip test structures using VACNT a) single electrode b) micro capacitor.

In the scope of this project two alternative strategies are presented. The first consist of on-chip grown VACNT coated by metal oxide (Figure 4). As it will be further discussed this approached needed to be paused due to technical issues with the equipment used for its development at the external research center.

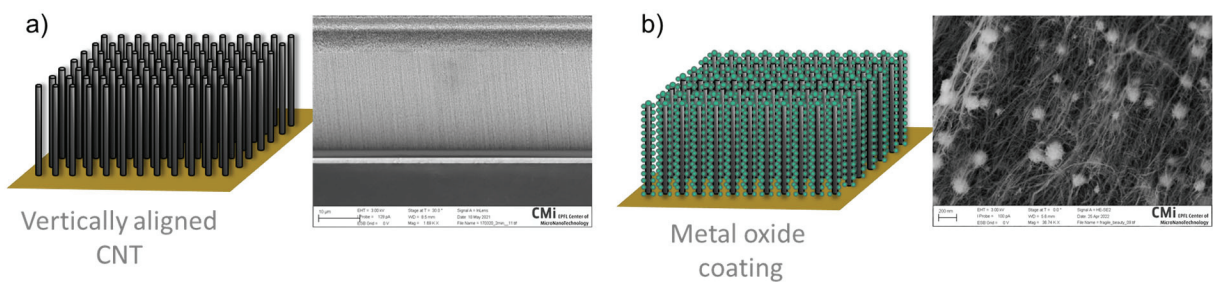


**Figure 4** Diagrams of the used electrodes and SEM pictures for a) vertically aligned carbon nanotubes (VACNT) and b) vertically aligned carbon nanotubes with metal oxide coating ( $\text{MnO}_2$ -VACNT).

The second alternative is founded on partially aligned CNT. Bundles of aligned CNTs are used as electrode material for ink-based electrode with the possibility of incorporating metal oxide particles to the ink formulation (Figure 5).

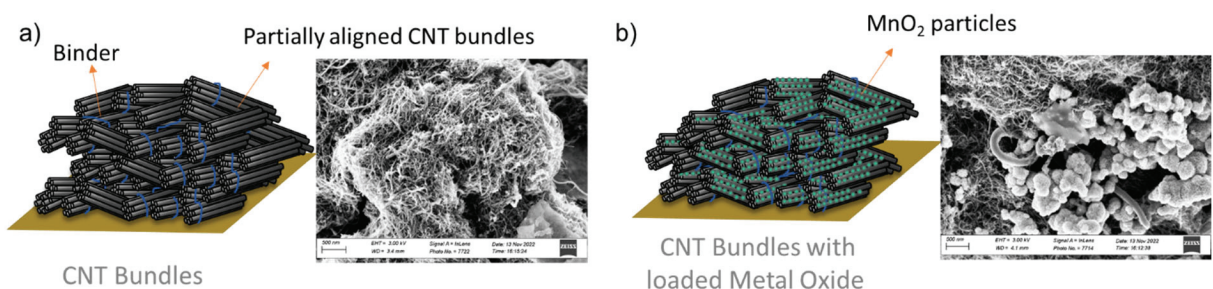


**Figure 5** Diagrams of the used electrodes and SEM pictures for a) carbon nanotube bundle electrodes (CNT-Bundles) and b) vertically aligned carbon nanotubes with metal oxide coating ( $\text{MnO}_2$ -CNT-Bundles).



## 2.2 Nanocarbon Electrodes Fabrication

### 2.2.1 CVD Growth of Carbon Nanotube Electrodes

The CNT growth was done in the Binnig and Rohrer Nanotechnology Center in IBM Zurich, using chemical vapor deposition (CVD). The CNT dense vertical forests are grown on the silicon chips grown directly on the current collector (Figure 6).

Test structures are continuously evaluated during all the critical steps and the performance metrics and test methods are summarized below:

- dense CNT forests- high porosity 4-10 nm; method: SEM
- high density  $0.85 \times 10^{12}$  CNT/cm<sup>2</sup>; method: SEM
- conformal coating pseudocapacitive materials; method: SEM
- electrical measurements: electrodes resistance, contact resistance.

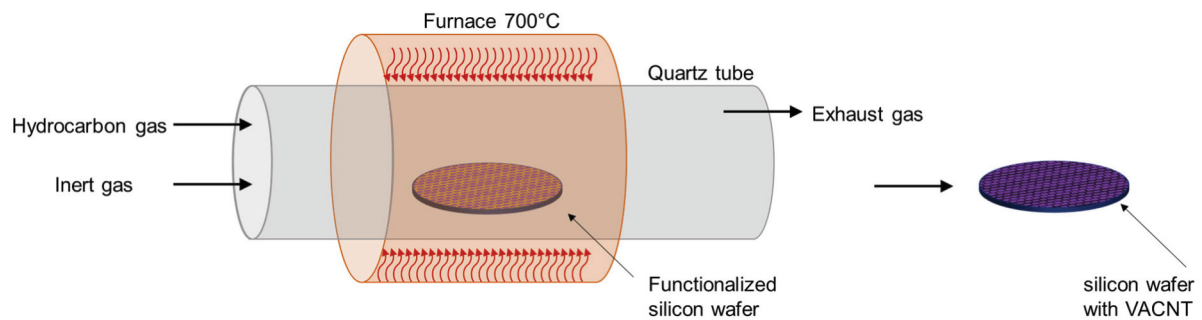


**Figure 6** Diagram represented VACNT grown on silicon substrate using a CVD system.

## 2.3 On-chip capacitors design optimization

We conducted a parametric study, optimizing the design of on-chip supercapacitors using test structures on Pt/RuO<sub>2</sub> to maximize the capacitance and minimize the resistance. We used different areas of baseline metal line electrodes and compared them with interdigitated supercapacitor structures and optimized space filling curve structures which have been shown to be the most efficient capacitor designs [28].

## 2.4 Pseudocapacitive layer integration

### 2.4.1 Electrochemical deposition

An important component of our technology to enlarge the current state of the art performance is the integration of a hybrid capacitive technology. This technology relies on ohmic charge accumulation, determined by the large surface area, and faradaic charge accumulation determined by electron transfer and charge intercalation.

One of the methods selected to incorporate the faradaic reaction component into the device is electrochemical deposition. This technique has the advantage to be cost effective and easily controllable since the deposited layer is controlled by the applied current or voltage and the precursor. Also, post-



treatment procedures are reduced because the deposition area is limited to the conductive region where the charge or current is applied.

In order to achieve a better understanding of the obtained layers the materials are first deposited on flat carbon surfaces to facilitate their chemical and physical characterization. After characterization and optimization on flat surfaces the most promising materials are transferred to high surfaced area carbon structures and the methodology is optimized and characterized again on the final structure.

#### 2.4.2 CNT-MnO<sub>2</sub> electrode preparation by mixing MnO<sub>2</sub> and CNT bundles

An alternative scalable and cost-effective method was developed. It will be benchmarked and compared to the VACNTs and electrochemical deposition mixing MnO<sub>2</sub> prepared by co-precipitation method at room temperature [29].

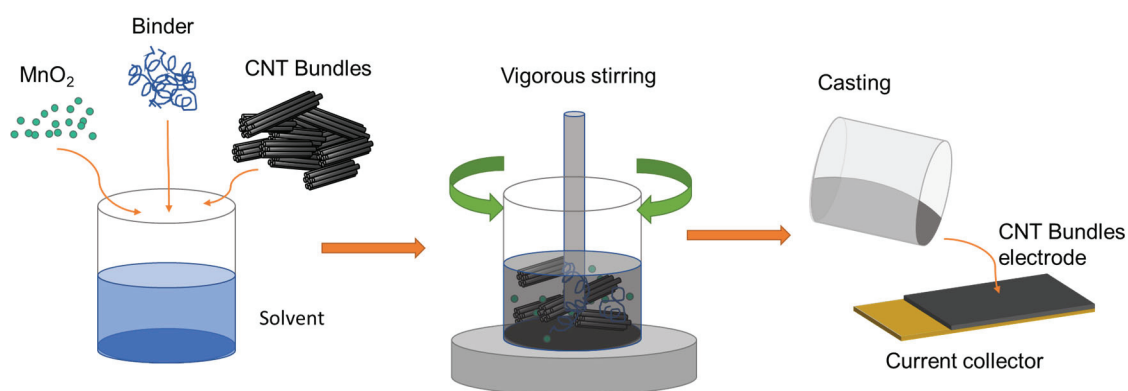


**Figure 7** Sketch representing the electrodes ink casting for CNT-Bundle electrodes with MnO<sub>2</sub>

The composite electrode was prepared by mixing the MnO<sub>2</sub> powder with the aligned carbon nanotube bundles in solvent and binder with a certain weight ratio. For capacitance comparison pristine carbon nanotubes bundle electrode were prepared with the same weight ratio of binder to active material. The polymer binder content was selected in order to provide good mechanical properties of the electrode. Electrodes were casted and pressed on the current collectors for testing. Figure 5 shows a sketched representation and detailed morphology of the casted electrodes and Figure 7 shows a sketch representation of the ink fabrication processed.

## 2.5 Electrochemical characterization

The performance evaluation is realized by electrochemical characterization. The characterization is comprised at two levels: (i) three electrode or half-cell measurement to evaluate the electrode materials, electrode/electrolyte interaction and components optimization process and (ii) two electrode or full-cell measurements to evaluate device performance (Figure 8).

The supercapacitor and electrode components are evaluated in terms of capacitance, voltage window, energy and power density, capacitance retention upon cycling and charge discharge dynamics.



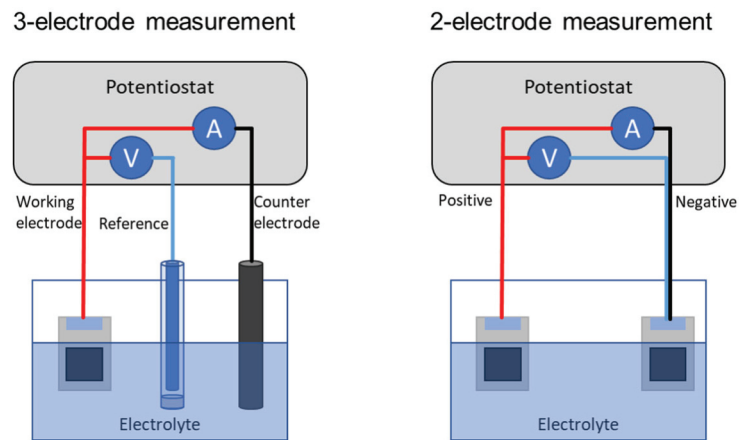


**Figure 8** Diagram representing the measurement set-up for the 2 different testing configurations.

The electrolytes development characterization consists of:

- determination of the voltage window by charge/discharge measurements
- ionic conductivity ( $10^{-2}$  S/cm) evaluation by electrochemical impedance spectroscopy
- performance determination at different temperatures and stability after temperature treatment between -20 and 80 °C by cyclic voltammetry.

The full test protocol consists of:

- Cyclic voltammetry at varying sweep rates
- Galvanostatic charge-discharge at varying current densities
- Electrochemical impedance spectroscopy
- Durability test upon continues charge-discharge cycling
- Determine cell discharge by galvanostatic charge discharge measurements.

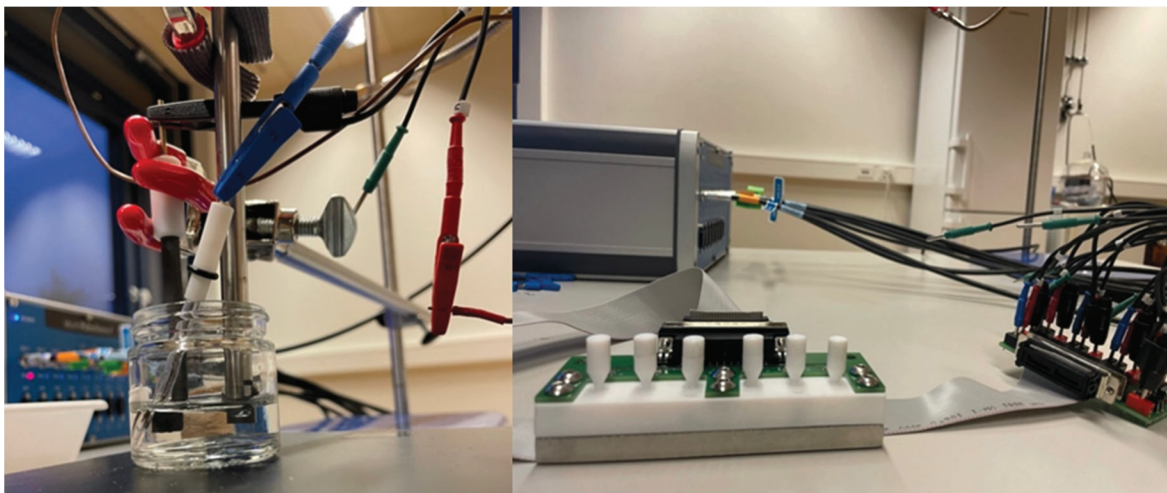


**Figure 9** Left: Standard electrochemical cell set-up, for 3-electrode measurements. Right: high throughput cell (6 channels) for on-chip supercapacitor measurements.



The electrochemical methodology and calculations of capacitance, energy, power and resistance were done according to the international standard IEC 62391-1 “Fixed electric double-layer capacitors for use in electric and electronic equipment - Part 1: Generic specification”. [30], [31]

The main test set-ups are shown in the image below. We designed and fabricated a custom electrochemical cell to test our devices in parallel, and seal them in order to be able to perform high throughput measurements outside the glovebox, as seen in Figure 9, right.

The full cell investigations were carried out at various temperatures in Swagelok cells (Figure 10) made of polytetrafluoroethylene with stainless steel (316L) current collectors. The filter paper with the thickness of 170  $\mu\text{m}$  (Whatman™) and diameter of 12 mm was used as the separator. The electrode material was prepared in form of 10 mm discs (geometric surface area: 0.785  $\text{cm}^2$ ) and placed on current collectors. All the components were afterwards soaked in electrolytic solution.

All the Swagelok cells tested with organic electrolytes were assembled in the glove box (Jacomex, France) under argon atmosphere with less than 1 ppm of  $\text{O}_2$  and  $\text{H}_2\text{O}$ .

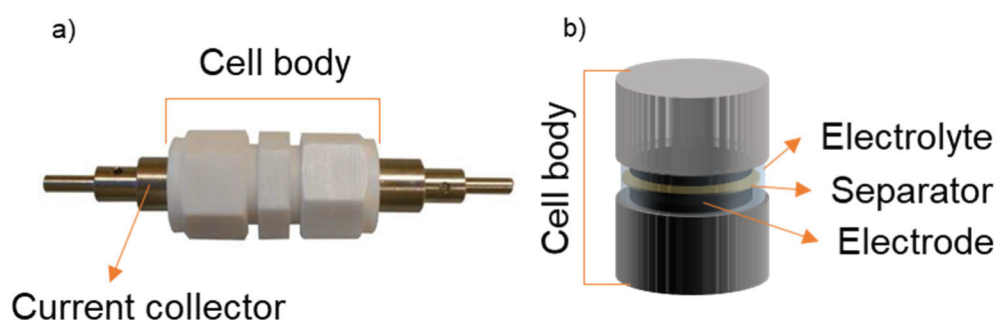


**Figure 10** Swagelok cell used for supercapacitor full cell tests (2-electrodes measurement) a) picture of the full cell b) detailed sketch of the cell body configuration.

## 3 Results and discussion

This section describes the qualitative and quantitative results achieved within the project describes the key findings and experiments made.

### 3.1 Decorated CNT electrodes and alternative electrodes

This section addresses work related to the optimization of the electrode material and contact with the current collector. We have to achieve a contact resistance in the range of 10  $\Omega$  for VACNT and to develop dense and scalable CNT arrays on conductive substrates.

#### 3.1.1 Determination of CNT forest density

We determine the electrodes density by the weight-gain method [32] Several samples were weighted with and without CNT using a Mettler Toledo (MS105DU) scale with a 0.01 mg readability to determine the area mass gain upon the CNT growth. Using the transmission electron microscopy (Talos F200S) at 200 kV in CIME center in EPFL (Figure 11). After analyzing CNT from several different samples, we determine the inner diameter of our in-house grown CNT to be in the range of 6 to 8 nm, and to have



between 2 and 3 walls. Considering these obtained values, we have determined the theoretical maximum possible forest density and calculated our average tube density and fill factor and summarize it in Table 1. Considering these data, and comparing them to the results presented by Esconjauregui et al. [32] the CNT forests are sufficiently dense and therefore the target was achieved.

Table 1 Calculation results for the CNT forest density determination

Scenario	Tube diameter [nm]	Number of walls	Theoretical maximum density [tubes.cm <sup>-2</sup> ]	Calculated density [tubes.cm <sup>-2</sup> ]
Minimum	6	2	$1.7 \times 10^{12}$	$4.4 \times 10^{11}$
Maximum	8	3	$2.8 \times 10^{12}$	$8.5 \times 10^{11}$

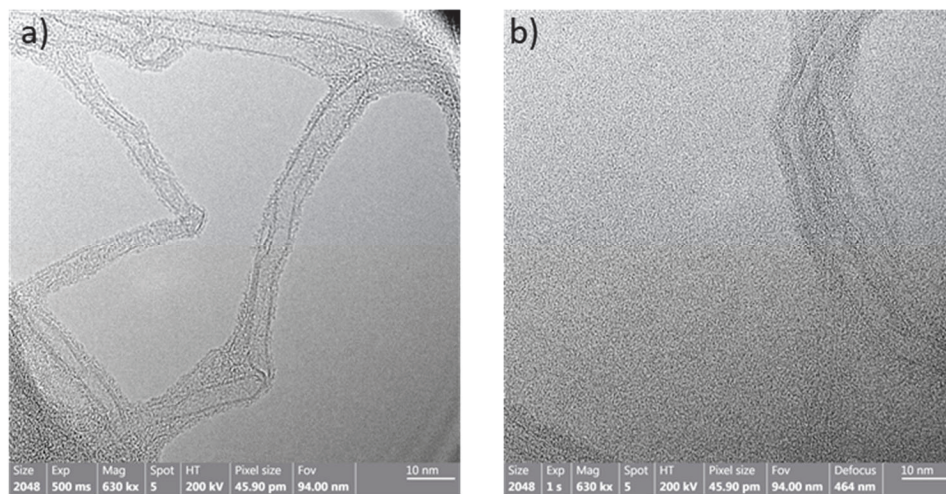
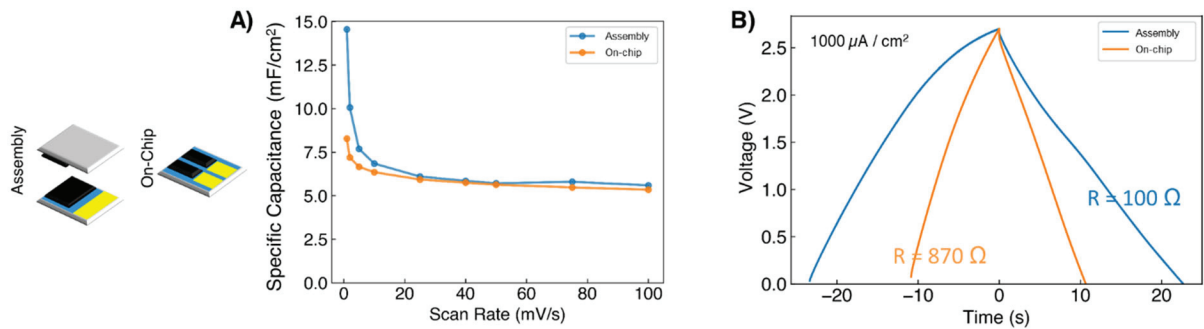


Figure 11 Transmission electron microscopy of in-house grown CNT. a) shows CNT with dual wall and inner diameter of 6 nm b) shows CNT with 3 walls and inner diameter of 6 nm.

### 3.1.2 Electrode design of micro-capacitor on-chip

The following process is used to fabricate our micro-supercapacitor devices on silicon wafers: the current collectors are made of metal, selected to obtained appropriate high density CNT growth, Chemical vapor deposition is used to create the CNT electrodes directly on the current collector, which then deposits metal oxide on the CNT surface. The manufacturing approach enables simple structuring, processing, and control of electrodes' height between a few micrometers and 100 micrometers as well as their porosity and density.

We began by comparing traditional sandwich structure with on-chip (planar design). The specific capacitance is derived from the curve of cyclic voltammetry (CV) measurements at different scan rates. The resistance of each device can be calculated from the IR drop of the galvanostatic charge discharge (GCD) measurements. In Figure 12, the miniaturized microcapacitors on chip have a comparable performance to the conventional sandwich device, despite the higher resistance of the planar devices.



**Figure 12** A) Specific capacitance at different scan rate. B) Through the IR drop of the charge-discharge curve, we can find the resistance of the device.

In order to decrease the resistance of the devices, we implemented various electrode architectures, as illustrated in Figure 13. The optimization of the interdigital electrodes was carried out with the aim of enhancing specific capacitance values while simultaneously decreasing resistance. Through these efforts, we were able to achieve a reduction of resistance by a factor of 4, while concurrently increasing capacitance by a factor of 2, showing a very promising path for miniaturized on-chip devices.

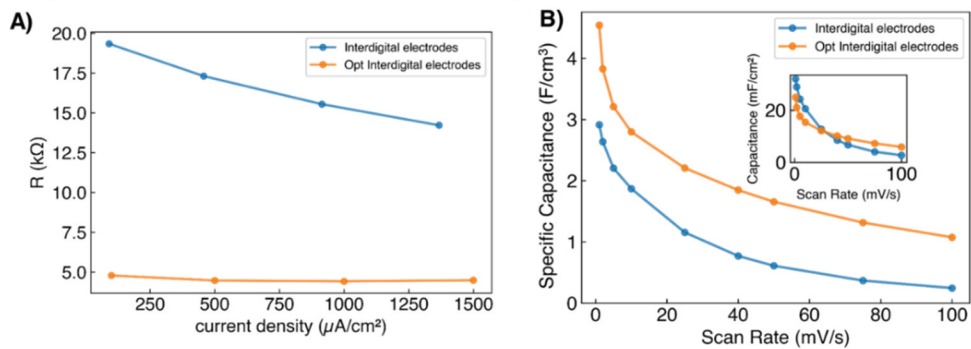


**Figure 13** Optimization of interdigital electrode A) the resistance vs. different current density. B) specific capacitance vs. different scan rates.

Compared to the other CNT on-chip technology, which applied layer-by-layer coating with conducting polymers on CNT [33] or inkjet-printing [34], our technology enables us to miniaturize the device size and fabricate different patterns on-chip. Table 1 shows the potential of the technology to achieve high-energy supercapacitors, even with unoptimized designs. The hindering factor in our case is the high resistance on-chip, due to the measurement set-up connections and the quality limitations of metals developed at the lab scale microfabrication facility. Measurements from [33] and [34] were done in 3-electrode setup with an excess of electrolyte, thus, the specific capacitance values are probably overestimated there than the one reported in our structures. Further research on the optimization of on-chip supercapacitors is needed. The following section shows the results of the influence of different current collector geometry.

Table 2 Comparison of CNT on chip technology

Electrode Material	Electrolyte	Specific Capacitance [mF/cm²]	Ref.
VACNT	Na <sub>2</sub> SO <sub>4</sub> -PVA gel	1300	[33]
SWCNT/ AC/Ag	[BMIM][BF <sub>4</sub> ]	100	[34]
<b>Our technology (VACNT)</b>	<b>[EMIM][BF<sub>4</sub>]</b>	<b>20</b>	



### 3.2 Thin film

The geometry of the current collector in a supercapacitor device plays a crucial role in determining its performance. In this study, we evaluated the impact of electrode geometry on performance by investigating various spacings between electrodes and different designs. As depicted in Figure 14A, our experimental results show a positive effect of the gap reduction between electrodes and the enhancement of the area capacitance of design A. However, only after a more aggressive gap miniaturization (design A: small gap, in blue) the improvement of specific capacitance was observed. The capacitances for middle gap (in orange) and large gap (in green) devices are comparable (with the experimental conditions playing a more important role than the gap itself). All these preliminary studies suggest that further device miniaturization is needed to improve specific capacitance.

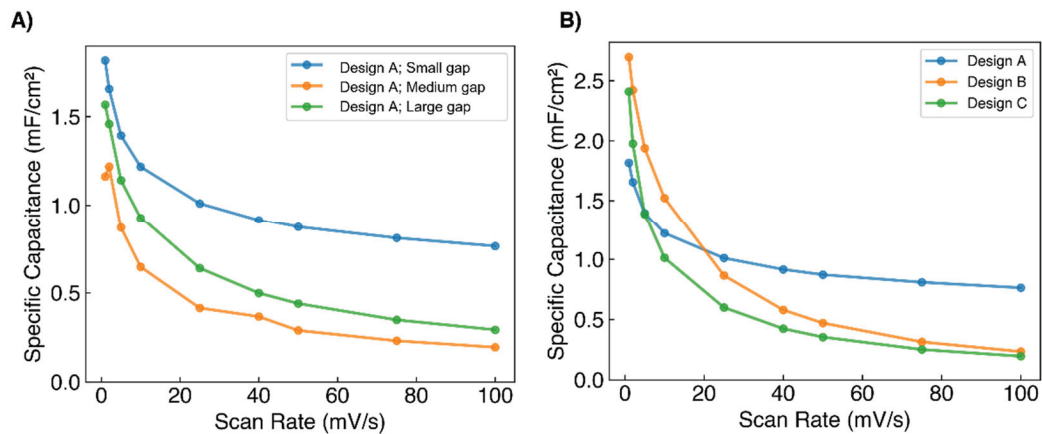


**Figure 14** Specific capacitance at different scan rates: a) The impact of the gap between design A on the areal capacitance and b) The comparison of areal capacitance for different design

Furthermore, our results, as seen in Figure 14B, indicate that while design B and design C have better performance at lower scan rates, design A has better performance at higher scan rates. To gain a deeper understanding of this behavior, we will conduct Electrochemical Impedance Spectroscopy (EIS) measurements. The EIS measurements provide information about the resistance, capacitance, and charge transfer kinetics of the system, which can help to understand the behavior of different electrode designs and how they impact the performance of the device.

Table 3 Properties of different test structures on-chip using 30 nm RuO<sub>2</sub> thin films, including energy density, specific capacitance, and resistance.

Sample	Energy density at 100 $\mu\text{A}/\text{cm}^2$ [ $\mu\text{Wh}/\text{cm}^2$ ]	Capacitance at 100 $\mu\text{A}/\text{cm}^2$ [mF/cm <sup>2</sup> ]	Capacitance at 10 mV/s [mF/cm <sup>2</sup> ]	Resistance [ $\Omega$ ]
Design A	0.118	0.85	1.22	43.8
Design B	0.027	0.20	1.20	49.1
Design C	0.030	0.21	1.01	76.3



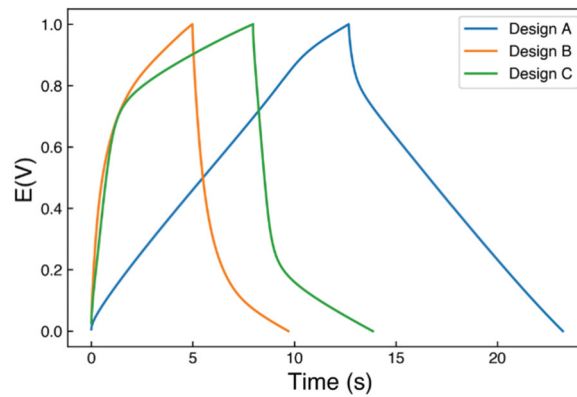


**Figure 15** Charge-discharge curves at a current density of  $100 \mu\text{A}.\text{cm}^{-2}$  showing the IR drop, a measure of the resistance of the supercapacitor device for different electrode designs.

As seen in Table 3 and Figure 15, resistance is a major issue for on-chip supercapacitors. Our comparison of CV and resistance obtained from charge-discharge curves, as shown in Figure 16A and B, reveals that design A have lower resistance at different current densities compared to design B. To further decrease resistance of the design B, we compared different amounts of digital numbers in design B and found that samples with 60 digital numbers had lower resistance, as seen in Figure 16C and D. Additionally, by reducing the gap between the electrodes as seen in Figure 16E and F we were able to increase specific capacitance.

Based on the results shown in Figure 16, we found that the design A has lower resistance due to its larger area per digit. To understand the influence of the gap and area, we kept the same length per digit, we have used widths of  $50 \mu\text{m}$  and  $20 \mu\text{m}$  and different gaps, and, we found that both effects are not dominant (Figure 17).

Additionally, we found that the contact of the measurement was not always stable, which affected the usability of the results for the report. Therefore, in order to obtain more reliable results, we are conducting new measurements with an improved measurement cell.



## Parametric Study

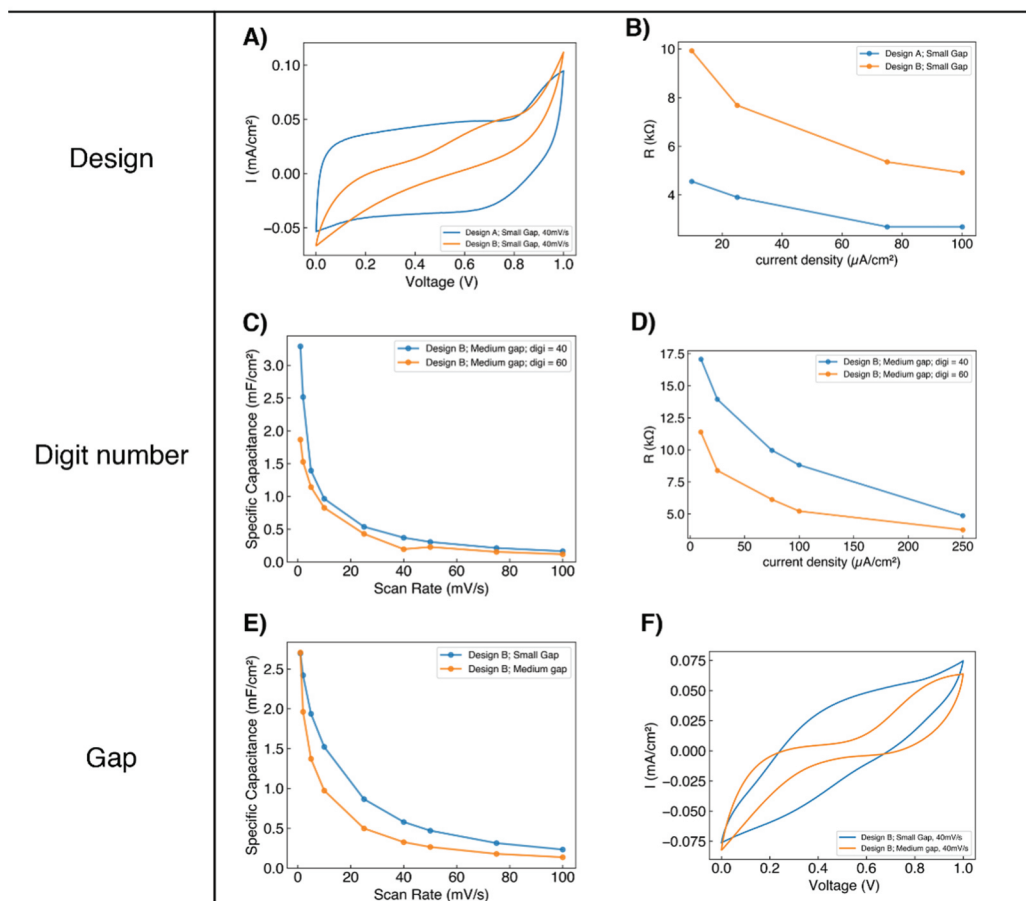


**Figure 16** Performance results of electrode design on-chip parametric study. On top of the figure, we compare design A against design B with the same gap showing A) CV curves at a scan rate of 40 mV.s<sup>-1</sup> and B) the resistance at different current densities. In the middle, we compare the influence of the number of digits in design B: C) the specific capacitance at different scan rates and D) the resistance at different current densities. At the bottom of the figure the influence of the gap in design B is shown in E) The specific capacitance at different scan rate and F) CV curve at 40 mV.s<sup>-1</sup>.

In conclusion, the geometry of the current collector, including the spacing between electrodes and the design of the electrodes, plays a crucial role in determining the performance of a supercapacitor device. By understanding the underlying electrochemical principles and utilizing appropriate designs, as well as utilizing analytical tools like EIS, it is possible to understand how to improve the performance of these devices. At this stage, in order to obtain a good performance for the devices, it is recommended to keep the design A and reduce the gap in between to have better specific capacitance. Another approach consists in increasing the number of the digits of the design B and decrease the gap. These are the main ways to improve the performance of supercapacitor devices and it is planned to continue this direction to optimize and improve above-mentioned designs. Additionally, we will also improve the measurement technique to have more accurate results.

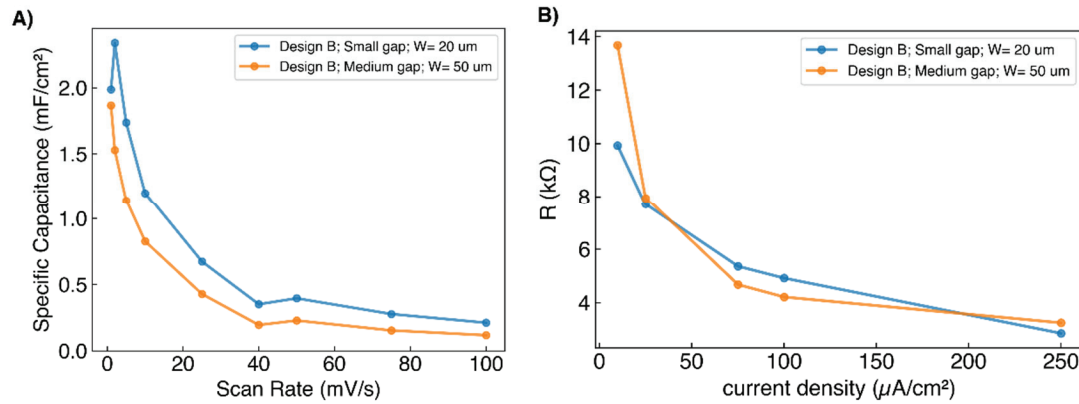


**Figure 17** The comparison of different interdigital electrodes geometries: a) the specific capacitance at different scan rates and b) the resistance at different current densities.

### 3.3 Electrode characterization

#### 3.3.1 Substrate influence on capacitance using standard electrolytes

During the initial evaluation phase for electrodes an aqueous electrolyte,  $\text{Na}_2\text{SO}_4$  1 M, was selected as standard electrolyte due to its accessibility, ease of use and compatibility with the tested substrates. This electrolyte has a high conductivity, is environmentally friendly and cheap, yet it cannot be considered for the final product due to its narrow voltage window and long-term compatibility issues with most commonly available on-chip packaging solutions.

There are several strategies for the design of micro capacitors on-chip. The most interesting one based on the patterned design by photolithography of electrodes on a Si wafer and consequent growth of VACNT. Nevertheless, this step is based on having a dense and well performing electrode by CNT growth on metal with is more complex than in Si. In order to evaluate the design viability and CNT addition to the substrate, modify CNT-growing conditions and modify contact resistance 3 different substrates has been tested: (i)  $\text{SiO}_2$ , (ii) highly doped Si (HiSi) and (iii) Si with a thin metal layer. The Cyclic Voltammetry results, and extracted capacitances are presented in Figure 18.

The characterization in aqueous system is a test process to easily understand the influence of the fabrication modifications on the CNT active area and performance capacitance while more complex electrolytes were being developed. In addition, the characterization in aqueous systems is important for the metal oxide deposition since most electrochemical deposition techniques and characterizations published in literature cover this kind of system giving us a good point for control and comparison.

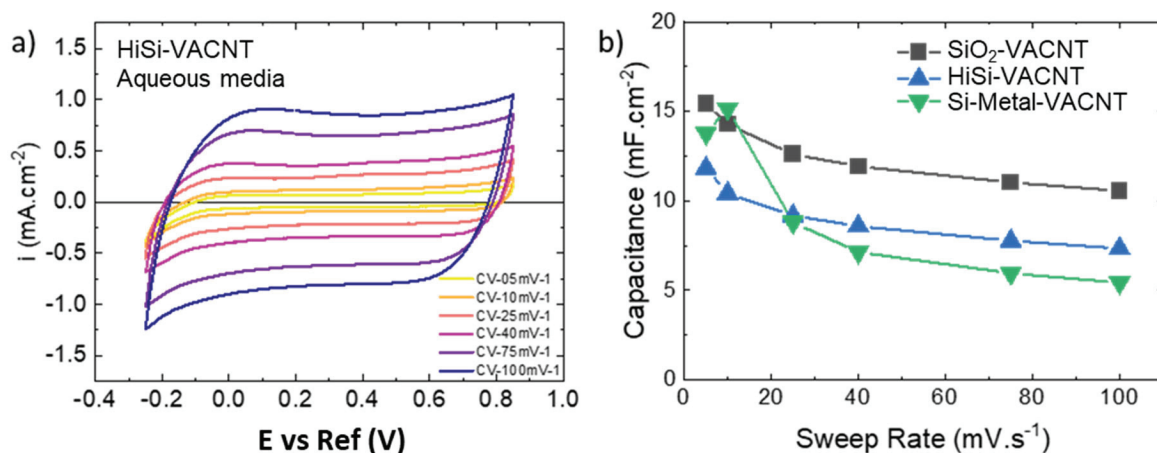


**Figure 18** 3-electrodes measurement results of a) Cyclic voltammetry results for a CNT electrode on highly doped Si measured in Na<sub>2</sub>SO<sub>4</sub> 1 M at 25 °C at 6 different sweep rates. b) Capacitance values from cyclic voltammetry at different sweep rates for 3 CNT electrodes on different substrates.

We have also studied the influence of the substrate using a commercial ionic liquid to establish the base performance of our standard electrodes (glassy carbon, graphene ink and Metrohm drop sense commercial electrodes) and then consecutively characterize the performance of our CNT-electrodes on said ionic liquid (Figure 19). The cyclic voltammetry for the 3-electrodes measurement results shows a much higher voltage window is enabled and larger capacitances are measured (around 40 mF.cm<sup>-2</sup> at 40 mV.s<sup>-1</sup>).

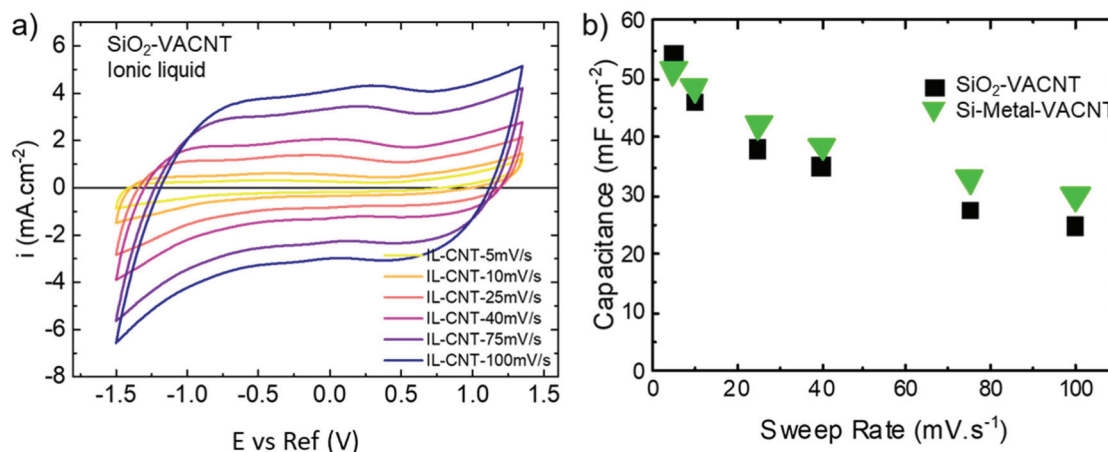


**Figure 19** 3-electrodes measurement results of a) cyclic voltammetry results for a CNT electrode on current collectors with CNT measured in an ionic liquid at 25 °C at 6 different sweep rates. b) capacitance values from cyclic voltammetry at different sweep rates for 2 CNT electrodes on different substrates.

Both of our tested standard electrolytes show good durability performance. In both cases, using aqueous electrolytes and ionic liquids the materials were cycled at least 1'000 times and, in both cases, the capacitance retention was above 85%, as shown in Figure 20b.

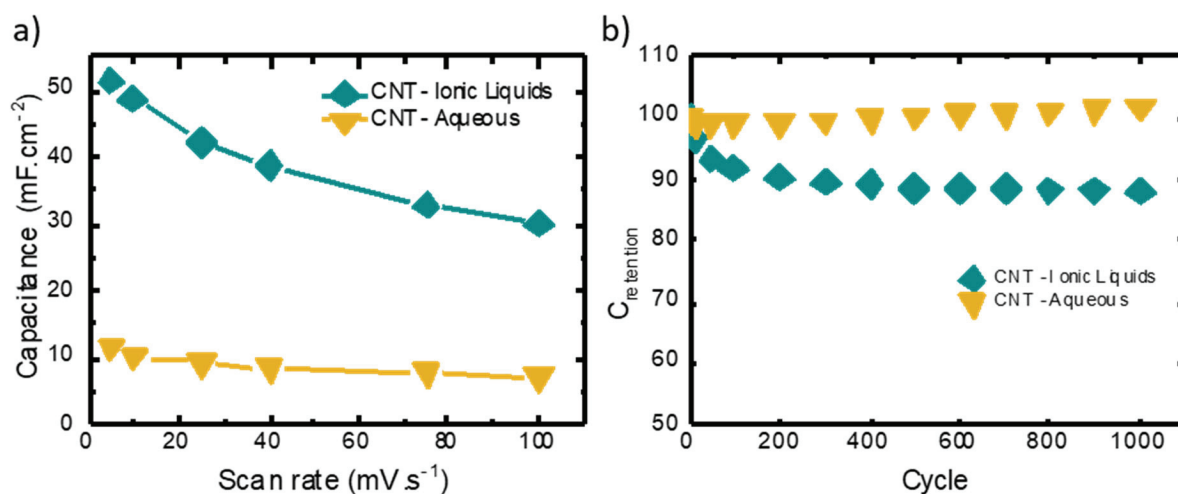


**Figure 20** a) Capacitance values from cyclic voltammetry at different sweep rates for 2 CNT electrodes on different electrolytes, aqueous and ionic liquids at 25 °C at 6 different sweep rates. b) Durability results showing the percentage of capacitance retention in comparison with the beginning of test, the electrodes were cycled 1'000 times and performance was evaluated every 100 cycles. Electrodes with capacitance performance retention over 85% are considered stable upon cycling.

### 3.4 Integration of Pseudocapacitive layer

Due to limitation on the required precursor necessary for ALD we decided to stop the activities on this alternative until a suited partner could be found. Instead, we first selected electrochemical deposition for the prototype and we evaluated different methods for process industrialization. Due to the difficulties encounter with the VACNT production and the elevated cost of the industrialization of electrochemical deposition on VACNT we also developed a solution based on ink of  $\text{MnO}_2$  particles and partially oriented CNT bundles. The details of the developed research are explained in the following sections.

#### 3.4.1 Optimization of metal oxide layers on flat model systems

Our technology is based on a hybrid capacitive response. This requires a pseudocapacitive layer, for our application we have selected to employ electrochemically deposited  $\text{MnO}_2$ . We have started this study on flat model surfaces, such as monolayer graphene or glassy carbon to facilitate characterization and understanding. Due to their morphology, these electrodes can be easily studied by physical characterization techniques as X-Ray diffraction (XRD), X-Ray photoelectron spectroscopy (XPS), energy-dispersive X-ray spectroscopy (EDX), profilometer and atomic force microscope (AFM). These types of characterization are beneficial to understand the depositions process, but they are not available when using the more complex system of the metal oxide on CNT-electrodes.

For the first approach we have selected to use short pulsed anodic deposition, since this methodology has the possibility to penetrate through the porosity of the CNT electrode due to the use of pulsed current and allows direct control of the deposited layer by control of the pulse time and applied current. As it can be seen in Figure 21a when the metal oxide is deposited on the glassy carbon a large capacitance increased is obtained.



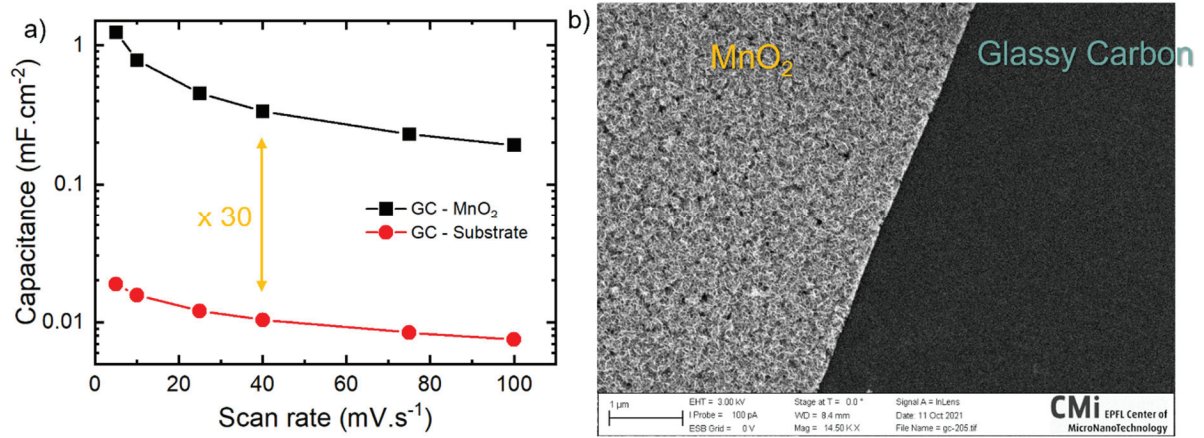


**Figure 21** a) Comparative capacitive response of glassy carbon substrate against electrochemically deposited on glassy carbon  $\text{MnO}_2$ . b) SEM image of the interface between the deposited pseudocapacitive layer and the glassy carbon substrate.

Once the methodology was established, we optimized the thickness of our two selected metal oxide materials, the  $\text{MnO}_2$  selected for its low cost, abundance and lower environmental impact as pseudocapacitive material for the final demonstrator.  $\text{RuO}_2$  was selected for the test structures on chip for its high performance and compatibility with clean room processes.

For this set of experiments, we varied the thickness of the deposited layer and found the optimum according to the obtained performance using a 3-electrode measurement set-up. Figure 22 shows the capacitive performance of the different types of metal oxide. For  $\text{MnO}_2$  no thicker layers than 500 nm could be deposited due to poor addition, and therefore this was selected as optimum and starting point for deposition on VACNT. For  $\text{RuO}_2$  no addition problems, nor stability issues were observed for the tested samples, therefore the 30 nm layer was selected for the optimization of the electrode structure on-chip described on Section 3.2.

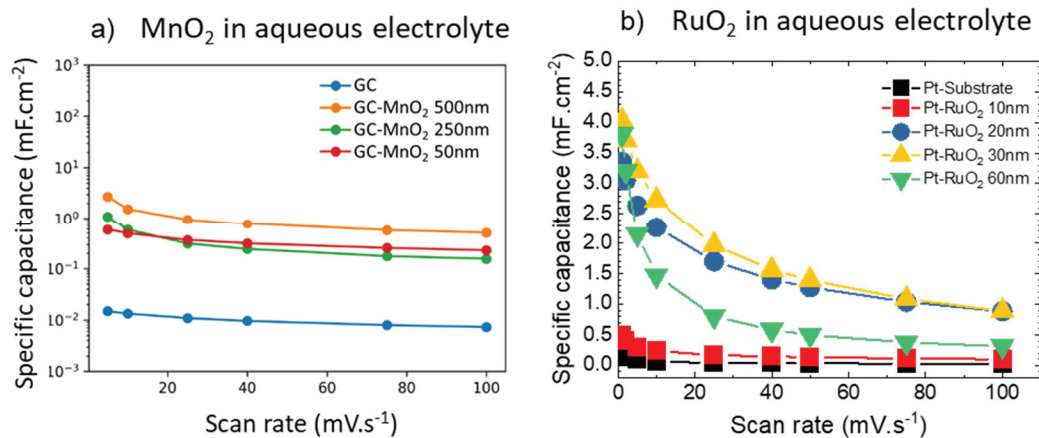


**Figure 22** Thickness optimization results for thin films of metal oxides on flat surfaces. a) Specific capacitance values from cyclic voltammetry at different scan rates for flat glassy carbon substrates with different  $\text{MnO}_2$  thickness layers. b) Specific capacitance values from cyclic voltammetry at different scan rates for platinum on silicon chips substrates with different  $\text{RuO}_2$  thickness layers. All experiments were performed in aqueous electrolytes at 25 °C and using a 0.8 V voltage window.



### 3.4.2 Metal oxide deposition on CNT electrodes

The next step after the investigation on flat surface is the deposition and characterization of  $\text{MnO}_2$  on rough electrodes. We successfully decorated VACNT with  $\text{MnO}_2$  and characterized them in aqueous electrolyte to ensure the efficiency of the coating using a 3-electrode measurement set-up. Figure 23 shows the results of the single electrode measurements where a specific capacitance of  $39.7 \text{ mF}\cdot\text{cm}^{-2}$  is achieved (at  $10 \text{ mV}\cdot\text{s}^{-1}$ ) showing an almost 10-fold increase compared to the VACNT without  $\text{MnO}_2$  ( $4.7 \text{ mF}\cdot\text{cm}^{-2}$  at  $10 \text{ mV}\cdot\text{s}^{-1}$ ).

Concerning the results obtained in 3-electrodes- set-up capacitor, usually the capacitance values are overestimated compared to 2-electrode measurements (full cell system). Despite the performance overestimation, the successful 3-electrode measurements give useful qualitative information about the activity of the incorporated oxide.

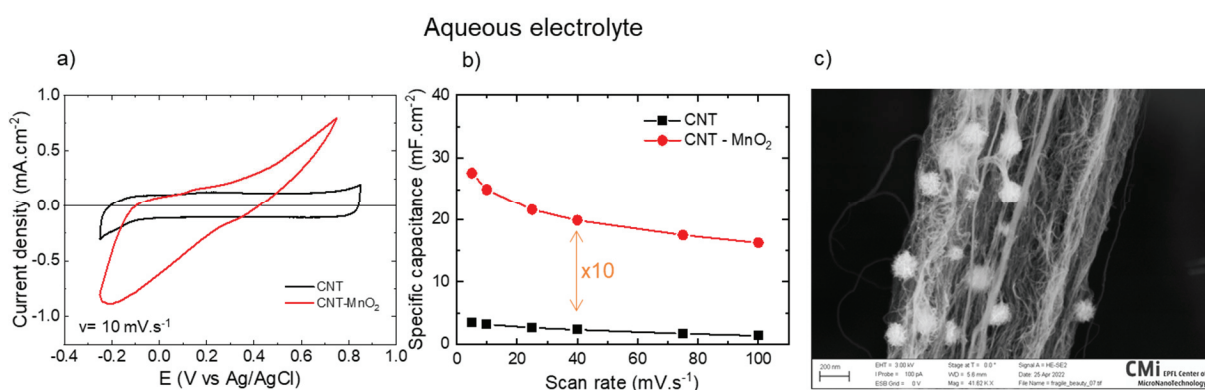


**Figure 23** a) Cyclic voltammetry of 3-electrode set-up at a scan rate of  $10 \text{ mV}\cdot\text{s}^{-1}$  comparing response of VACNT against electrochemically deposited  $\text{MnO}_2$  on VACNT b) Capacitive response of the same electrodes at different scan rates. All experiments were performed in aqueous electrolyte at  $25^\circ\text{C}$  using a  $1 \text{ V}$  voltage window. c) SEM image of the deposited pseudocapacitive particles and the VACNT electrode after testing.

## 3.5 Electrolyte development

The work related in this section targets the integration and optimization of electrolytes. As well as the description of the fabrication of a prototype of a full energy storage cell. Comprised of pseudocapacitive coated CNT arrays with liquid electrolyte.

The electrolyte is an important and often overlooked component of supercapacitors, its physical properties and interaction with the electrode will determine the performance and durability of the supercapacitor. In this area, we perform 3 complementary lines of research:

1. Test of standards electrolytes on CNT-electrodes to investigate and understand the influence of the modification on the materials of the electrode in performance.
2. Formulation and development of more complex electrolytes and their physical and electrochemical characterization on test substrates.
3. Integration of complex electrolytes with CNT-electrodes.



### 3.5.1 Gel electrolytes integration

The first set of experiments tested on this research line were aqueous based gels using poly(vinyl alcohol) (PVA) and an aqueous solution of sodium sulfate. In order to control the viscosity and evaluate the conductivity of the gels different formulations were tested.

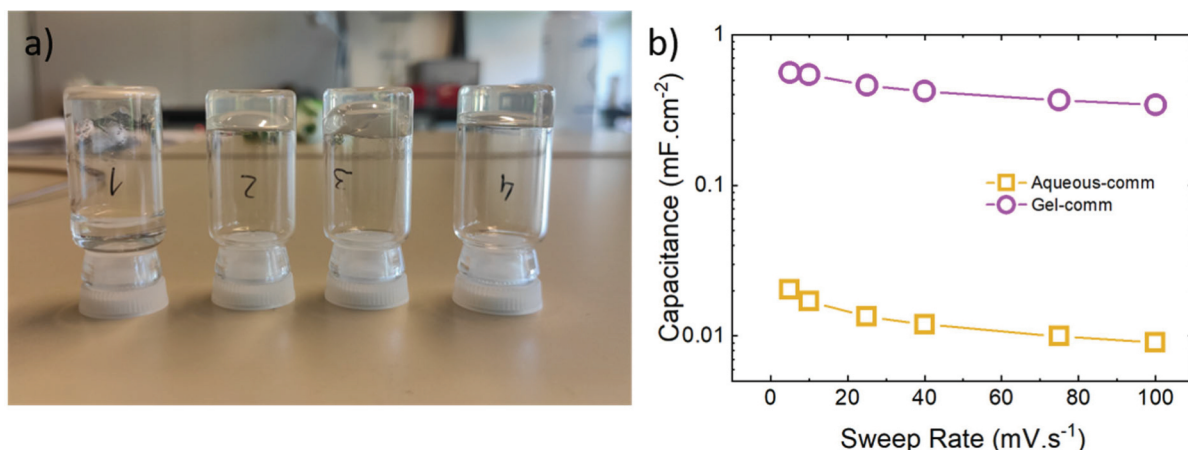


**Figure 24** a) Examples of 4 tested gels: Formulation 1. (on the left) does not form a gel, it has two separate phases solid and liquid. Formulations 2. 3. and 4. (from left to right) form gel and have increasing viscosities. b) Results comparing standard aqueous electrolyte vs. PVA gel on commercial test electrodes (-comm).

We obtained good results when testing the gel electrolyte on a standard carbon electrode, finding the right gel formation and higher capacitance values than in liquid form as shown in Figure 24. These results were not transferable to the CNT electrodes. Considering the large variability between samples (Figure 25a) and in some cases poor stability (Figure 25c) we concluded that gel electrolytes could not be optimized using standard electrodes, in contrast with the results on liquid electrolytes. In addition, higher capacitance values were obtained with liquid electrolytes when CNT electrodes were employed (Figure 25b).

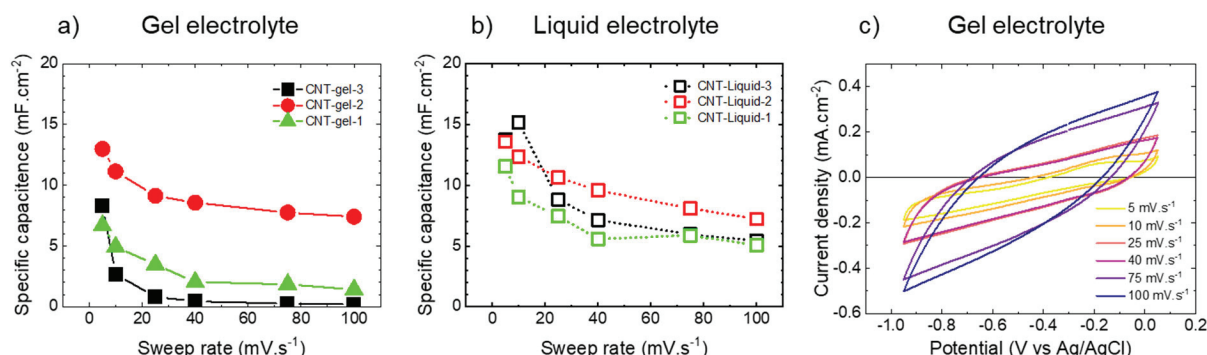


**Figure 25** Performance comparison between gel and liquid electrolyte. a) Reproducibility for specific capacitance values from cyclic voltammetry at different scan rates for 3 CNT electrodes on gel aqueous electrolytes and b) for aqueous liquid electrolyte. c) Cyclic voltammetry results for CNT-gel-2 electrode measured on gel electrolyte at 25 °C at 6 different sweep rates.

Although gel electrolytes promise to have larger voltage windows and higher operational temperature range, liquids electrolytes have shown higher capacitance and stability, and offer a cheaper and simpler processing for cell assembly. In addition, liquids electrolytes have shown good agreement between standard carbon electrodes and VACNT electrodes which allowed us to investigate electrolytes and



pseudocapacitive coatings on test structures. These results can then be translated to the VACNT. Taking these results into account we decided to stop further research in gel electrolytes and substitute it with liquid electrolytes.

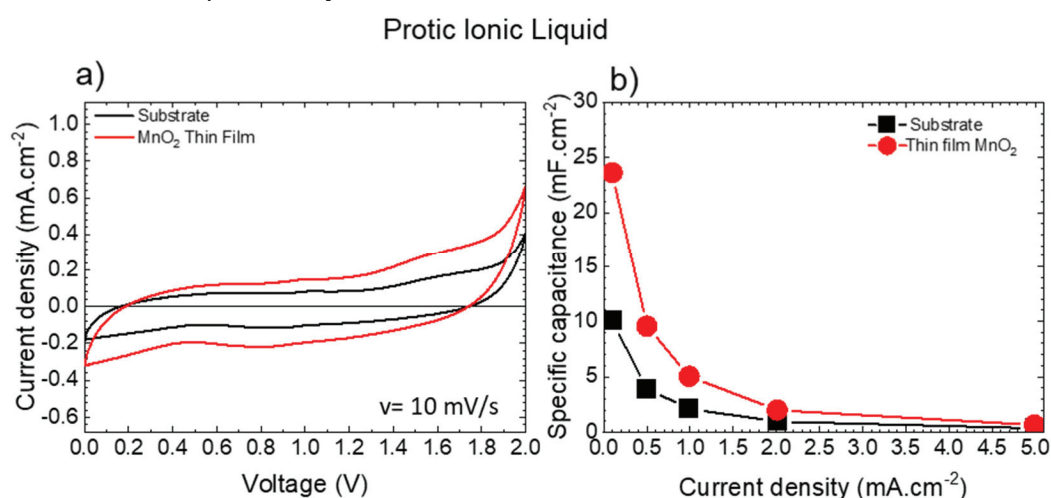
Here in Table 4 we present a comparison matrix for the theoretical performance values of the used electrolytes throughout our research.

Table 4 Comparison matrix for the theoretical parameters of the electrolytes presented through the report.

Electrolyte	Voltage window [V]	Temperature range [°C]	Conductivity [mS.cm <sup>-1</sup> ]	MnO <sub>2</sub> activity
Aqueous	1.2 V	0 - 100	90	High
Ionic Liquid	3.6 - 4 V	15 - 200	14.1	None
Protic Ionic Liquid	3.4 V	RT - 200	4	Low

### 3.5.2 Compatibility of Pseudocapacitive layer and electrolyte

One of the key aspects to evaluate when developing a supercapacitor with a pseudocapacitive layer is to select the correct medium to promote the reaction. MnO<sub>2</sub> is not active in most ionic liquids, therefore we have selected a commercial protic ionic liquid and evaluated the activity of our electrochemically deposit MnO<sub>2</sub> on a flat stainless-steel test substrate using a 2-electrode configuration with a standard carbon material as complementary electrode.



**Figure 26** Performance comparison of flat surfaces with and without MnO<sub>2</sub> in protic ionic liquid using a 2-electrode set-up. a) Cyclic voltammetry results measured at 25 °C at 10 mV.s<sup>-1</sup>. b) Specific capacitance results measured by galvanostatic charge discharge at different current densities at 25 °C normalized by cell footprint area.

As previously explained, tests on flat surfaces are the first step when adding metal oxide coatings. As shown in Figure 26, the activity of MnO<sub>2</sub> in protic ionic liquid is lower than in aqueous electrolyte as expected since the concentration of protons (necessary for the pseudocapacitive response) is lower in this medium. Yet a maximum 2.4 capacitance improvement can be observed (at 0.1 mA.cm<sup>-2</sup> the plain substrate has a specific capacitance of 10 mF.cm<sup>-2</sup> against the thin film MnO<sub>2</sub> which has 24 mF.cm<sup>-2</sup>). The use of ionic liquids offers a higher operational voltage and temperature

The next step on this research line was to compare the full cell activity testing the VACNT with MnO<sub>2</sub> in protic ionic liquids. Our current results on the addition of MnO<sub>2</sub> to the VACNT presented in Figure 27 show no capacitance improvement by the incorporation of the pseudocapacitive layer. The long-term





performance experiments (Figure 27c) show that the system is stable up to 20'000 cycles. The standard loss of performance criterium are a 20 % initial capacitance fade or a resistance increase larger than 50 %.

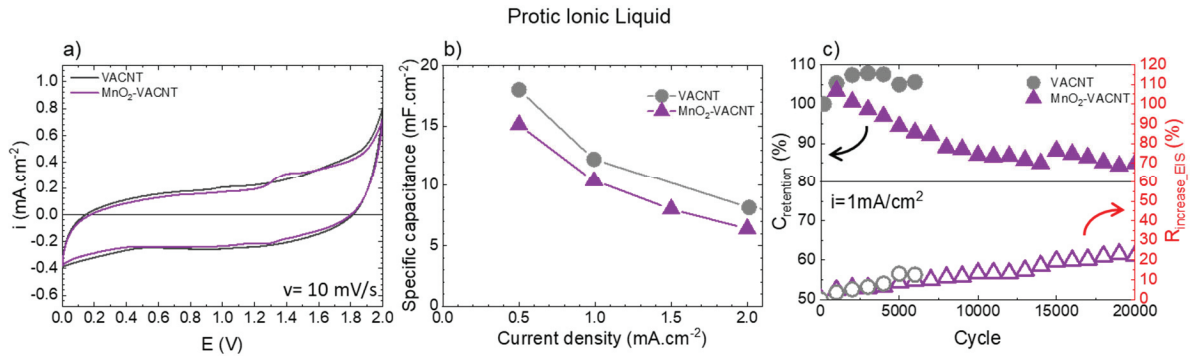


**Figure 27** Performance comparison of untreated VACNT and with MnO<sub>2</sub> coating in protic ionic liquid using a 2-electrode set-up. a) Cyclic voltammetry results measured at  $10 \text{ mV.s}^{-1}$ . b) Specific capacitance results measured by galvanostatic charge discharge at different current densities. c) Long-term performance (on-going tests) at  $1 \text{ mA.cm}^{-2}$  for full cells with VACNT and MnO<sub>2</sub> coated VACNT. All measurements were performed at  $25^\circ \text{C}$  normalized by cell footprint area with a voltage window of 2 V.

Our main hypothesis is that our current MnO<sub>2</sub> loading, in the order of  $70 \mu\text{g}$ , is not sufficient to have a positive effect on capacitance and we are dedicating our efforts on improving the coating on the VACNT electrodes using two different approaches: (i) by improving the coating distribution and (ii) by increasing the coating load in order to have a viable methodology for the on-chip VACNT whenever the CNT grow system is available again.

We were able to produce complex VACNT structures and we have validated the VACNT micro capacitor on-chip as shown in section 3.1. We have improved our measurement system to better record impedance spectroscopy data, and we performed thin film test structures to optimize the final design of the electrodes.

On sections 3.4 and 3.5 we have described our progress on VACNT electrochemically coated with MnO<sub>2</sub> using protic ionic liquids. We have not finalized this demonstrator. Our efforts are on improving the coating load and distribution to be able to have a system compatible with the VACNT. Nevertheless, during the last year of this project the chemical vapor deposition tool at BRNC (IBM) that we use for the growth of VACNT broke down and has been out of order since. Alternative sources of carbon nanotubes were required for the supercapacitor electrodes and two successful alternatives were found:

1. Commercial vertically align carbon nanotubes grown on conductive silicon wafers.
2. In house prepare ink-based electrodes composed of partially oriented carbon nanotubes (CNT-Bundles) and binder.

These two solutions allowed us to continue the validation of technology. In the case of the commercial VACNT we will use them for material development and electrolyte compatibility validation. We use this alternative to optimize the materials and processes using VACNT and once the production is re-established, to be able to produce a demonstrator as the one targeted at the beginning of the project.



### 3.6 Overview of supercapacitor demonstrator and tests of figures of merit obtained with an ink casted CNT Bundles electrode

As a full capacitor solution, we offer a more economical and simple manufacturing technology using CNT bundles electrodes. The necessity of alternative carbon sources opened up a different route of fabrication based on ink electrodes and allow us in spite of these previous shortcomings to present here a full energy storage solution based on partially aligned carbon nanotubes bundles loaded with  $\text{MnO}_2$  in protic ionic liquid. Which is a more economical and easier to produce solutions and has yield the highest performance metrics.

#### 3.6.1 Supercapacitor demonstrator with partially aligned nanotubes bundles with $\text{MnO}_2$ in protic ionic electrolyte

We concluded that the most scalable and low-cost method, promising for process industrialization consists of electrode using VACNT bundles loaded with  $\text{MnO}_2$ . Our developed ink can be deposited on the substrates by printing or standard coating methods used in industry. The full energy storage systems were tested both in aqueous medium for validation and organic medium as demonstrator using a Swagelok cell. A comparison of the capacitive performance with the same testing conditions is presented in Figure 28.

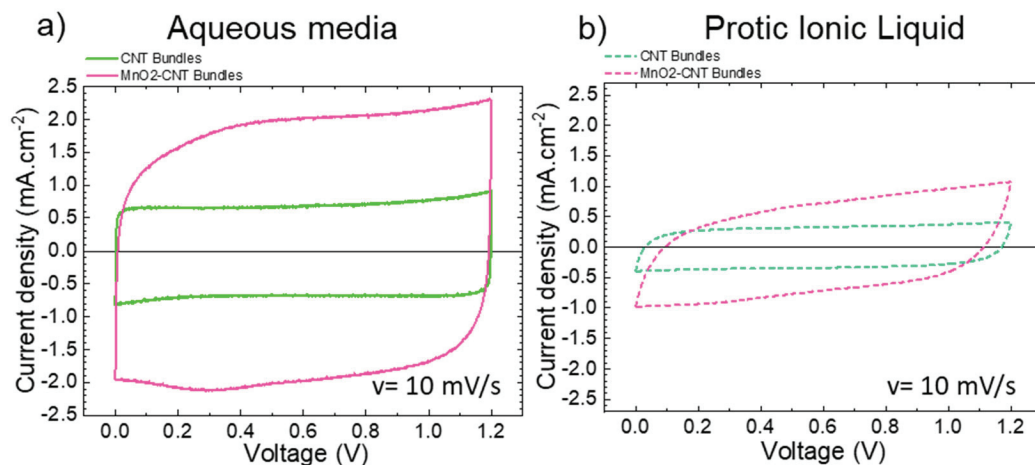


**Figure 28** Cyclic voltammogram of CNT bundles capacitor with (pink curve) and without (green curve)  $\text{MnO}_2$  in a) aqueous electrolyte b) organic electrolyte.

As seen from Figure 28, and contrasted in section 0, there is a higher current response with  $\text{MnO}_2$  addition independently on the electrolyte. The larger response in aqueous media is related to the  $\text{MnO}_2$  activity, as well as much higher conductivity values, therefore obtained capacitance is higher as well as CV profile is more rectangular than in organic medium.



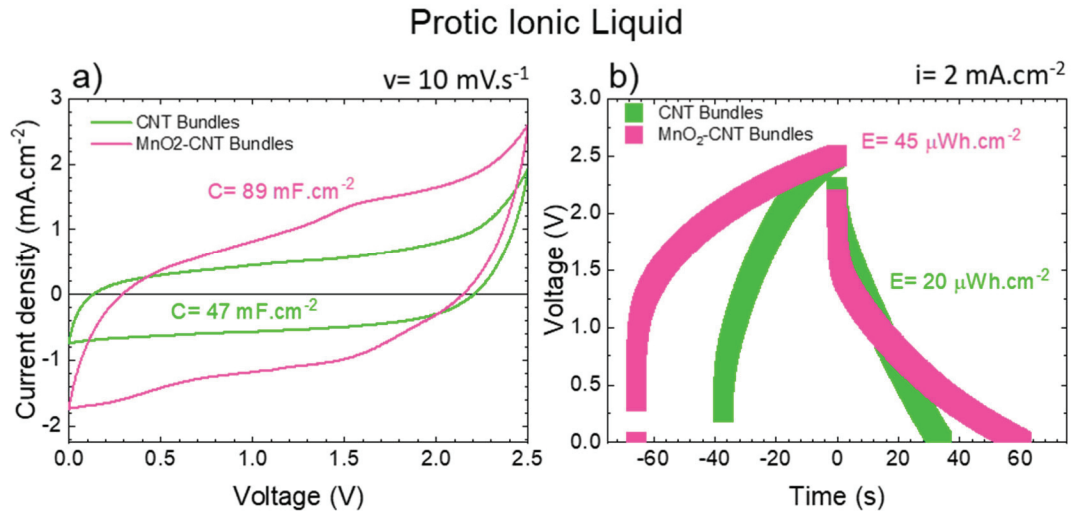


**Figure 29** Comparative performance of CNT-Bundle electrodes at 2.5V in protic ionic liquid a) cyclic voltammogram at room temperature and 10  $\text{mV.s}^{-1}$  and b) galvanostatic charge discharge

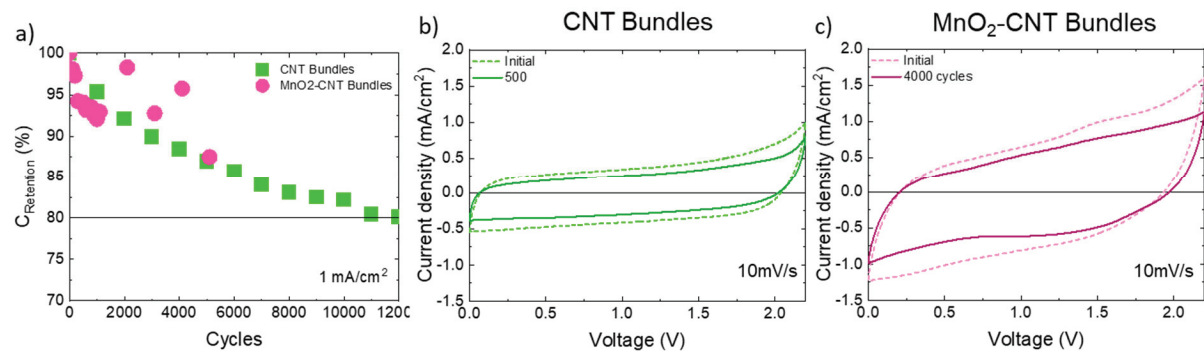
However, recorded activity of pseudocapacitive layer in organic medium is still a challenging topic in the energy storage field. Therefore, the currently recorded current density increase with MnO<sub>2</sub> in organic medium is the main highlight of this project. Figure 29 and Table 5 presents our highlight results for full cell test of all the presented technologies.

Table 5 Comparative performance metrics of presented CNT capacitor technologies. Data recorded at 2  $\text{mA.cm}^{-2}$

Electrode type	Electrolyte	Voltage window [V]	Capacitance [ $\text{mF.cm}^{-2}$ ]	Energy density [ $\text{μWh.cm}^{-2}$ ]	Power density [ $\text{mW.cm}^{-2}$ ]	Resistance [ $\Omega$ ]
CNT Bundles	Aqueous	1.2	77	18	1.3	2
CNT Bundles	Protic ionic liquid	2.5	23	20	2.1	32
MnO <sub>2</sub> -CNT Bundles	Aqueous	1.2	108	21	1.2	2
MnO <sub>2</sub> -CNT Bundles	Protic ionic liquid	2.5	51	45	1.9	28

### 3.6.2 Durability

The durability test for the CNT-bundles electrodes is undergoing, Figure 30 shows the results obtained so far. The plain CNT-Bundles electrodes show acceptable performance up to 12'000 cycles. The measurements for MnO<sub>2</sub> containing electrodes are less evolved at the moment and only 5'000 cycles have been recorded due to set-up limitations. So far, the performance is stable and above the commonly reported performance of end of life at 3'000 cycles [29], [31].



**Figure 30** Durability performance for the CNT-Bundles electrodes with and without MnO<sub>2</sub>. a) Shows the capacitance retention upon continuous cycling for both tested systems. Loss of performance criteria is reached when more than 80 % capacitance is lost. Cyclic voltammetry results for initial and last recorded CV curve for b) CNT-Bundles and c) CNT-Bundles with MnO<sub>2</sub>.

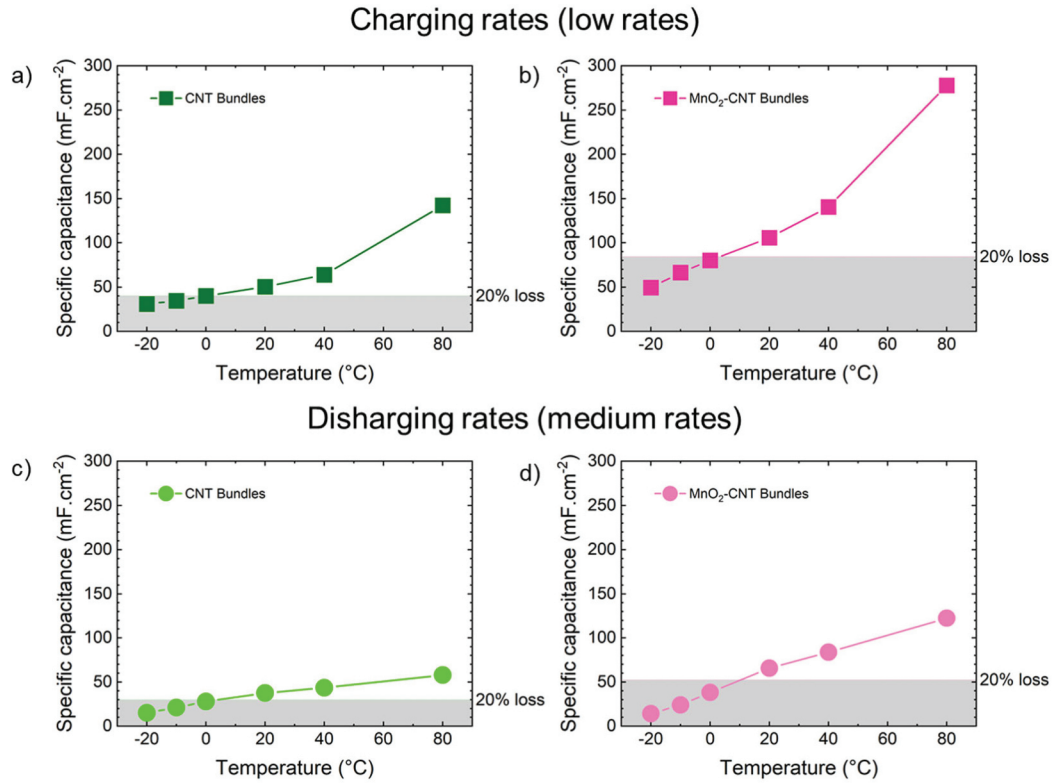
Even though the measurements are not completed, two different strategies are being explored to improve the current durability performance: (i) optimize the electrode synthesis with more adequate tools for ink casting and formulation (ii) reformulation of the current use electrolyte to help stabilize the metal oxide, expand the voltage window and temperature range.

### 3.6.3 Performance under different temperatures

The performance of the presented electrochemical capacitor based on partially oriented CNT-Bundles was tested at temperatures ranging from -20 °C to 80 °C following the European space agency specifications on energy storage devices. The measurements were designed to test the performance under a certain temperature and the stability of the device after operation at the given temperature.

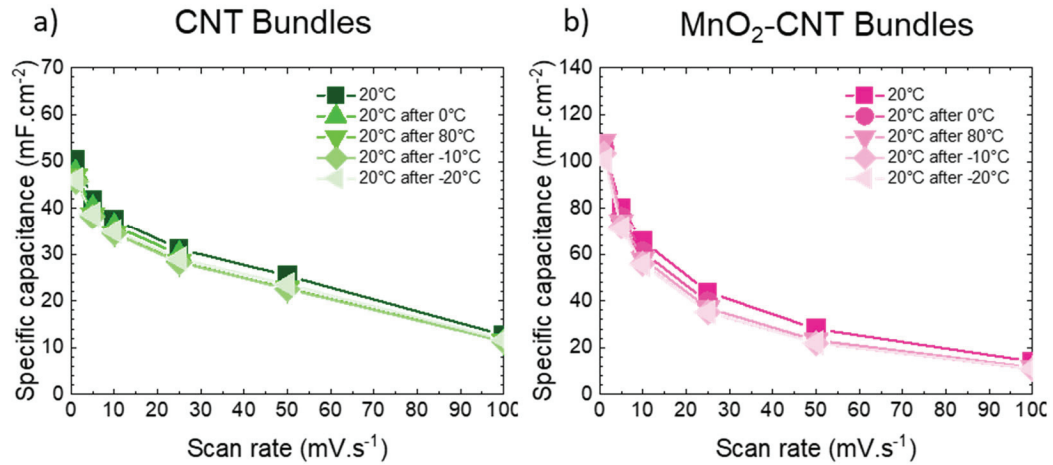
The measurements were performed at National Institute for Research and Development in Microtechnologies IMT in Bucharest, Romania. The same cells were tested at all selected temperatures. The temperature was controlled using a climate chamber and the cells were conditioned for 90 min at the selected tested temperature prior to the start of the electrochemical characterization. After the electrochemical characterization at a selected temperature measurement was performed, the cells were tested again at 20 °C to assess the performance stability.

Figure 31 shows the influence of temperature in the specific capacitance of the two different electrodes at different current densities. Both systems can operate within the whole range of temperatures, performing both hot and cold starts. Nevertheless, for both systems the performance drops below 80 % -of the initial capacitance at 20 °C- for temperatures lower than -10 °C. Therefore, the measured operative temperature range is from 0 to 80 °C.



**Figure 31** Electrochemical performance measured by specific capacitance for 3 different scan rates at different temperatures. The dotted lines represent the 20 % capacitance loss (in reference to values at room temperature) for each scan rate. a) Values for CNT-Bundles at low scan rates and b) Values for CNT-Bundles with MnO<sub>2</sub> at low scan rates, c) Values for CNT Bundles at medium scan rates and d) Values for CNT-Bundles with MnO<sub>2</sub> with medium scan rate.

The second part of the experiment consisted of measuring the performance after each temperature test. As it can be seen in Figure 32 no performance loss was observed after the temperature treatment. The tested cells show no irreversible damage after the measurement time was of 12 days of consecutive temperature experiment treatments.



**Figure 32** Characterization of the stability of the electrochemical performance after each temperature measurement showing the specific capacitance at 20 °C at different scan rates for the a) CNT-Bundles and b) CNT-Bundles with MnO<sub>2</sub>.

Although the cells cannot operate with less than 80 % capacitance loss at the full targeted temperature range from -20 to 80 °C, they can operate from 0 to 80 °C and it is possible to operate them at -10 and -20 °C (with a maximum of 50 % specific capacitance loss) and perform cold starts. It is also highly significant that no irreversible damage was recorded after the full temperature test. All these results area a good indication that with a better packaging strategy the full operational range is within reach.

### 3.7 Benchmark results with state-of-the-art solutions

The CNT Bundle electrodes of electrode were used due to the technical difficulties with VACNT growth in BRNC and the lack of alternatives until February 2023. Nevertheless, it showed a promising boost of energy density by using MnO<sub>2</sub> in combination with protic ionic liquid which is a new area of research in the field. Here we present a comparative table of merit for similar type of electrodes as the CNT Bundles. It is important to highlight that in contrast with our presented solution were full cell electrochemical capacitors were tested most of these materials are tested using 3-electrodes measurements and have only asses the viability of the material.

Table 6 Benchmarking data for state of the art nanocarbon technologies in electrochemical capacitors. Highlighted in green they are the results from this project.

Electrode type	MnO <sub>2</sub> -CNT Bundles	MnO <sub>2</sub> -CNT Bundles	MnO <sub>2</sub> -CNT composite [35]	MnO <sub>2</sub> -Carbon fibers [36]	MnO <sub>2</sub> -CNT [37]	MnO <sub>2</sub> flakes-CNT Composites [38]
Electrolyte	Aqueous	Protic ionic liquid	Aqueous	Aqueous	Aqueous gel	Aqueous
Voltage window [V]	1.2	2.5	0.6	0.8	1.8	1.0
Specific Capacitance [mF.cm <sup>-2</sup> ]	108	51		312	39	3500
Energy density [μWh.cm <sup>-2</sup> ]	21	45		244	4	94



Power density [mW.cm <sup>-2</sup> ]	1.2	1.9		6.3	598	193.0
Resistance [Ω]	2	28	2.5	1.4	20	
Specific Capacitance [F.g <sup>-1</sup> ]	5.4	2.6	34.5	50.0	56.0	
Energy density [Wh.kg <sup>-1</sup> ]	1.04	2.3	1.7	22.6	6.0	
Power density [W.kg <sup>-1</sup> ]	59.6	97.5	34.5	1000	870	
Temperature	0°C to 80°C	0°C to 80°C	RT	RT	RT	RT
Cycle life	Under test	4000*	200	10000	100	10000

Although the test on VACNT were interrupted it is our VACNTs supercapacitors have yielded 10 Wh/kg which is a SOA result, showing promise for the approach initially proposed in this project as the VACNTs will allow a more uniform nanoscopic metal oxide coating leading to an increased energy density.

### 3.8 Fabrication Scaling and Cost Assessment

The fabrication scalability of fabrication of CNT supercapacitors depends on several factors, including the method of CNT synthesis, the technique used for depositing the CNTs onto the substrate, and the design of the supercapacitor.

We use scalable fabrication methods, standard in the IC industry, such as chemical vapor deposition (CVD) which was shown to be scalable for large-scale production of CNTs in roll-to-roll processes. However, the cost and efficiency of these methods can vary.

Depositing CNTs onto a substrate can also affect scalability. Techniques such as drop-casting and spin-coating can be relatively simple, cheaper and scalable, but may not provide as high of a CNT density as the direct growth developed here. Therefore, a trade-off has to be considered for products industrialization.

The design of the supercapacitor can also impact scalability. For example, using a 3D architecture with aligned CNTs grown vertically can increase the active surface area and improve performance, but may be more difficult to fabricate at scale compared to a 2D design or the bundled CNT devices.

Currently, the cost of supercapacitors is relatively high compared to other energy storage technologies. They currently cost significantly more than batteries, whose costs range from \$100 to \$1,000 per kWh compared to \$5,000 to \$10,000 per kWh for supercapacitors. The main reason for this is the high cost of materials used in the production of supercapacitors, such as activated carbon, carbon aerogels, CNTs and graphene, which are not yet available on a large scale or cost-effective and the lower energy density, of 5 - 10 Wh/kg compared to 100 – 250 Wh/kg for Li-ion batteries.

In order to achieve a cost of less than \$100 per Wh/kg for supercapacitor fabrication, several factors must be considered like the development of more cost-effective materials for the electrodes. We are addressing this issue by using CNTs which can be produced with 1 \$/kg and cheap and abundant metal oxide pseudocapacitive materials.



Another important factor is the scale of production. As production volume increases, costs per unit typically decrease due to economies of scale. However, achieving large scale production requires significant investment in equipment and facilities, which will be the main barrier to achieving low costs per Wh/kg.

Due to the use of standard batch semiconductor processes, we roughly estimate a cost of 3\$/cm<sup>2</sup> with an energy density of 1mWh/cm<sup>2</sup> for a production of 500'000 pieces. There is a potential possibility to scale down to 1\$/cm<sup>2</sup> when scaling to volumes of more than 100 Million pieces per year, which is a competitive cost for the consumer electronics market.

### 3.9 Dissemination and Communication

This section addresses the evaluation of the prototype with potential lead customers for the medical, consumer and self-powered IoT sensors use cases and validation our Go-To-Market strategy.

The final demonstrator of the capacitor cell consisted of a 1 cm<sup>2</sup> hybrid CNT/MnO<sub>2</sub> supercapacitor, with an ionic liquid electrolyte. Specifications: 50 mF, 30 Ω, 100 mA, 2.5 V. The plan was to use it to power a temperature and humidity sensor.

The customer feedback activities were slightly reduced, due to the delay in the final prototype and only partial achievement of certain figures of merit and involved mainly exchanges with Sensirion and ST Microelectronics by Ms. Moldovan. Some preliminary discussions with potential customers such as ST Microelectronics, Sensirion, Renault, Peugeot, were carried out to discuss the design features and needed prototypes.

The outcome of the IMD project:

- suggested go-to-market strategies:
  - Energy storage for renewable energies for the grid.
  - Energy storage for factory robots.
- investors meeting was cancelled due to covid travel restrictions.

A market study of microbatteries and their applications was performed together with Sensirion SA, investigating the potential of our technology to replace microbatteries and if there is an interesting market potential.

### 3.10 Interaction with the Industrial Advisory Board

We have established an Industrial Board of Advisors (IAB) consisting of:

- Dr. Johannes Schumm, VP RD, Sensirion AG, Switzerland,
- Dr. Andreas Wild, former Executive Director of the ECSEL,
- Dr. Stéphane Monfray, Project and Group Leader, Silicon Technologies Development, STMicroelectronics, Crolles, France,
- Dr. Elise SAOUTIEFF, project manager at CEA-LETI.

It is worth noting that Mr Roland Brueniger, Programme Manager of the research programme in Electricity Technology, in the Swiss Federal Office of Energy, SFOE, attended as well the IAB meetings as an observer.

The Industrial Advisory Board had a first kick-off meeting in October 2021, and as discussed in the kick-off we followed up individually with the IAB members on more detailed discussions depending on their respective expertise in February and September 2022. The conclusions are summarized below:





- For powering an integrated circuit like a microcontroller, one can envision a supercapacitor with a footprint of 2 mm<sup>2</sup> with less than 1mW power capability (100 μW is enough for many IoT applications), with a cost of less than 1 \$ per 2 mm<sup>2</sup>.
- The global IoT market is expected to have an annual growth rate of 10.53% during 2022-2027. With the current global situation and severe issues regarding electricity, gas and energy consumption, there is an increased need for monitoring the consumption of energy and gas more than ever. This is resulting in an increased adoption of monitors for smart buildings and stores, where changing the batteries is a hurdle, therefore autonomous energy solutions are required. However, it was difficult to precisely estimate the market for such specific applications.
- Integration with harvesters is a promising application for start-ups as the market is very fragmented and niche applications can constitute a good entry point to the market.

The 2<sup>nd</sup> Industrial Advisory Board meeting was organized as an online meeting on November 21st, 2022. In this meeting the technical progress concerning the supercapacitor technology (in large part reflected in this report) has been presented. We also reported the applied mitigation strategies, the deviations and the achievements reflected in the status of milestones and deliverables of the project.

The IAB Board was involved in the discussions related to the tasks on customer feedback on prototype and on markets, which helped the project to reduce the planned expenses on these items and to progress with a dual-path that included both a scaled VCNT process evaluation and a final demonstrator based on inks of bundles of commercial CNTs mixed with MnO<sub>2</sub>, which were internally characterized.

The IAB concluded that enough progress has been made to continue exploring the potential of the proposed approach, but the data does not seem to highlight an area in which the solutions developed will stand out so far from other existing approaches. The TRL level achieved was estimated at TRL= 2-3 while to further engage industrial partners, a TRL = 4 (technology validated in the laboratory) would be needed. The topic of research is highly multidisciplinary and difficult, in a competitive international framework; the merit of the team is that they were able to come close to the state of the art in the field in limited time frame and identify promising directions of future R&D.

## 4 Conclusions

Within this project we were able to achieve: (i) highly dense vertically aligned carbon nanotubes forest grown on a metal substrate and (ii) inks based on bundles of CNTs and MnO<sub>2</sub>. Various developments allowed us to create adaptable and optimized cell and VACNT electrode designs on-chip using photolithography techniques. This is a crucial step in order to obtain miniaturized electrochemical capacitors. Moreover, we optimized the device design for on-chip miniaturized electrochemical capacitor using scalable microfabrication techniques.

On the other hand, the final demonstrator cell was not based on the VACNTs due to unexpected shut down of the equipment needed for such CNT electrode fabrication. The final supercapacitor cells have been evaluated on electrodes based on inks of bundles of commercial CNTs mixed with MnO<sub>2</sub>, and compared with VACNTs/patterned metal lines - this technology is scalable but at other scale compared with an on-chip technology that could benefit from advanced lithography methods and etching. On the other hand, the cost of this option is much lower and may address applications on flexible substrates.

We have also been able to incorporate ionic liquids with MnO<sub>2</sub> enlarging so the voltage operation of the composite between carbon nanotubes and metal oxide. This progress enables the possibility to have full cell operation at temperature for 0 to 80 °C and, full performance recovery, after operating the cells in a range from -20 to 80 °C.



The electrolyte used in the demonstrator is a commercial ionic liquid showing best performance and stability with our tested electrodes. This combination allows a larger voltage window operation per cell and a better temperature stability.

In conclusion, we developed and measured a proof of concept of a full-cell electrochemical capacitor system using carbon nanotubes bundles and ionic liquids, establishing pseudocapacitive response with an enlarged voltage operational window, performance loss lower than 20 % for temperatures from 0 to 80 °C and full performance recovery when operating at temperatures from -20 to 80 °C, with environmentally friendly components and low-cost processes.

## 5 Outlook and next steps

This research project has generated a deeper knowledge about the development of the electrode and electrolyte and their integration and about some potentially promising avenues for the future. The next steps will include:

- There is a continuation of the research on energy storage technologies in Nanolab-EPFL on alternative on-chip CNTs supercapacitor designs, material innovations and on-chip energy storage demonstrator answering to industrial specifications, which could constitute the basis for various industrial exploitation paths when more maturity will be reached.
- Development of an industrial prototype in the electrochemistry lab LIMNO, EPFL focusing on high energy density electrodes materials and novel supercapacitor designs supported by an Innogrant mechanism at EPFL (Clara Moldovan and Victoria Manzi).
- As recommended by the IAB we will consider updating the strategy for commercialization depending on results (additional ~6 months probably needed for an optimized prototype); business development and fundraising will be done in the next 6 months to support process industrialization and validate the go-to-market strategy.

---

**Disclaimer:** EPFL-Nanolab and professor Ionescu have no involvement in the creation of the start-up Swistor SA, which uses the same name of this project and was created independently by Dr. Clara Moldovan in September 2022.

---

## 6 National and international cooperation

*National collaboration:*

Laboratory of Photonics and Interfaces (LPI) Institute of Chemical Sciences and Engineering (ISIC)  
Head of the Laboratory: Professor Michael Graetzel for electrolytes and pseudocapacitive layers know-how transfer and access to a full electrochemical testing facility.

*International collaboration:*

National Institute for Research and Development in Microtechnologies IMT – Bucharest, Romania for reliability and temperature testing



## 7 Publications

- Hung-Wei Li, Victoria Manzi, Sadegh Kamaei Bahmaei, Pooya Dehghan, Ali Saeidi, Clara F. Moldovan, and Adrian M. Ionescu, “*Vertical CNT Supercapacitors for 3D Integration of On-Chip Energy Storage*, *Micro and Nanoengineering Conference*”, Turin, Italy, September 2021. Oral presentation.
- Hung-Wei Li, Victoria Manzi-Orezzoli, Justyna Piwek, Adrian-Mihai Ionescu, Clara-Fausta Moldovan, “*Microsupercapacitors: Scaling Down and Electrode Architecture Optimization*”. International Symposium on Enhanced Electrochemical Capacitors (ISEECAP 2022) Bologna, Italy 11-15.07.2022 Poster presentation.
- Justyna Piwek, Victoria Manzi-Orezzoli, Hung-Wei Li, Adrian Mihai Ionescu, Clara-Fausta Moldovan, “*Redox-enhanced Vertically Aligned Carbon Nanotubes as the Novel Electrode Material for Microcapacitors*”. International Symposium on Enhanced Electrochemical Capacitors (ISEECAP 2022) Bologna, Italy 11-15.07.2022 Poster presentation.
- Hung-Wei Li et al., On-chip miniaturized supercapacitors Design and Optimization, Journal article in preparation, 2023.

## 8 References

- [1] L. L. Zhang and X. S. Zhao, “Carbon-based materials as supercapacitor electrodes,” *Chem. Soc. Rev.*, vol. 38, no. 9, pp. 2520–2531, Aug. 2009, doi: 10.1039/B813846J.
- [2] A. Balducci et al., “High temperature carbon–carbon supercapacitor using ionic liquid as electrolyte,” *Journal of Power Sources*, vol. 165, no. 2, pp. 922–927, Mar. 2007, doi: 10.1016/j.jpowsour.2006.12.048.
- [3] C. Largeot, C. Portet, J. Chmiola, P. L. Taberna, Y. Gogotsi, and P. Simon, “Relation between the ion size and pore size for an electric double-layer capacitor,” *J. Am. Chem. Soc.*, vol. 130, no. 9, p. 2730, Mar. 2008, doi: 10.1021/ja7106178.
- [4] S. G. Kandalkar, D. S. Dhawale, C. K. Kim, and C. D. Lokhande, “Chemical synthesis of cobalt oxide thin film electrode for supercapacitor application,” *Synth. Met.*, vol. 160, no. 11–12, p. 1299, Jun. 2010, doi: 10.1016/j.synthmet.2010.04.003.
- [5] Z.-S. Wu, X. Feng, and H.-M. Cheng, “Recent advances in graphene-based planar micro-supercapacitors for on-chip energy storage,” *National Science Review*, vol. 1, no. 2, pp. 277–292, Jun. 2014, doi: 10.1093/nsr/nwt003.
- [6] G. Xiong, C. Meng, R. G. Reifenger, P. P. Irazoqui, and T. S. Fisher, “A Review of Graphene-Based Electrochemical Microsupercapacitors,” *Electroanalysis*, vol. 26, no. 1, pp. 30–51, 2014, doi: 10.1002/elan.201300238.
- [7] W. Gu and G. Yushin, “Review of nanostructured carbon materials for electrochemical capacitor applications: advantages and limitations of activated carbon, carbide-derived carbon, zeolite-templated carbon, carbon aerogels, carbon nanotubes, onion-like carbon, and graphene,” *WIREs Energy and Environment*, vol. 3, no. 5, pp. 424–473, 2014, doi: 10.1002/wene.102.
- [8] J. Tao, N. Liu, L. Li, J. Su, and Y. Gao, “Hierarchical nanostructures of polypyrrole@MnO<sub>2</sub> composite electrodes for high performance solid-state asymmetric supercapacitors,” *Nanoscale*, vol. 6, no. 5, pp. 2922–2928, Feb. 2014, doi: 10.1039/C3NR05845J.
- [9] S. Iijima, “Helical microtubules of graphitic carbon,” *Nature*, vol. 354, no. 6348, Art. no. 6348, Nov. 1991, doi: 10.1038/354056a0.
- [10] M. S. Dresselhaus, G. Dresselhaus, and A. Jorio, “Unusual Properties and Structure of Carbon Nanotubes,” *Annual Review of Materials Research*, vol. 34, no. 1, pp. 247–278, 2004, doi: 10.1146/annurev.matsci.34.040203.114607.



- [11] R. Saito, G. Dresselhaus, and M. S. Dresselhaus, "Electronic structure of double-layer graphene tubules," *Journal of Applied Physics*, vol. 73, no. 2, pp. 494–500, Jan. 1993, doi: 10.1063/1.353358.
- [12] M. S. Dresselhaus, G. Dresselhaus, and R. Saito, "C60-related tubules," *Solid State Communications*, vol. 84, no. 1, pp. 201–205, Oct. 1992, doi: 10.1016/0038-1098(92)90325-4.
- [13] J.-P. Issi, L. Langer, J. Heremans, and C. H. Olk, "Electronic properties of carbon nanotubes: Experimental results," *Carbon*, vol. 33, no. 7, pp. 941–948, Jan. 1995, doi: 10.1016/0008-6223(95)00023-7.
- [14] T. W. Ebbesen, H. J. Lezec, H. Hiura, J. W. Bennett, H. F. Ghaemi, and T. Thio, "Electrical conductivity of individual carbon nanotubes," *Nature*, vol. 382, pp. 54–56, Jul. 1996, doi: 10.1038/382054a0.
- [15] E. Frackowiak, "Carbon materials for supercapacitor application," *Phys. Chem. Chem. Phys.*, vol. 9, no. 15, pp. 1774–1785, Apr. 2007, doi: 10.1039/B618139M.
- [16] L. Su, X. Zhang, C. Yuan, and B. Gao, "Symmetric Self-Hybrid Supercapacitor Consisting of Multiwall Carbon Nanotubes and Co–Al Layered Double Hydroxides," *J. Electrochem. Soc.*, vol. 155, no. 2, p. A110, Dec. 2007, doi: 10.1149/1.2806844.
- [17] P. Lu *et al.*, "Ternary composite Si/TiN/MnO<sub>2</sub> taper nanorod array for on-chip supercapacitor," *Electrochimica Acta*, vol. 248, pp. 397–408, Sep. 2017, doi: 10.1016/j.electacta.2017.07.162.
- [18] A. Lamberti, M. Fontana, S. Bianco, and E. Tresso, "Flexible solid-state Cu<sub>x</sub>O-based pseudo-supercapacitor by thermal oxidation of copper foils," *International Journal of Hydrogen Energy*, vol. 41, no. 27, pp. 11700–11708, Jul. 2016, doi: 10.1016/j.ijhydene.2015.12.198.
- [19] M. F. El-Kady *et al.*, "Engineering three-dimensional hybrid supercapacitors and microsupercapacitors for high-performance integrated energy storage," *Proceedings of the National Academy of Sciences*, vol. 112, no. 14, pp. 4233–4238, Apr. 2015, doi: 10.1073/pnas.1420398112.
- [20] Z. Su *et al.*, "Co-electro-deposition of the MnO<sub>2</sub>–PEDOT:PSS nanostructured composite for high areal mass, flexible asymmetric supercapacitor devices," *J. Mater. Chem. A*, vol. 1, no. 40, pp. 12432–12440, Sep. 2013, doi: 10.1039/C3TA13148C.
- [21] L. Qin *et al.*, "Polymer-MXene composite films formed by MXene-facilitated electrochemical polymerization for flexible solid-state microsupercapacitors," *Nano Energy*, vol. 60, pp. 734–742, Jun. 2019, doi: 10.1016/j.nanoen.2019.04.002.
- [22] J. Lee, J. Y. Seok, S. Son, M. Yang, and B. Kang, "High-energy, flexible micro-supercapacitors by one-step laser fabrication of a self-generated nanoporous metal/oxide electrode," *J. Mater. Chem. A*, vol. 5, no. 47, pp. 24585–24593, Dec. 2017, doi: 10.1039/C7TA07960E.
- [23] R. Guo *et al.*, "In-Plane Micro-Supercapacitors for an Integrated Device on One Piece of Paper," *Advanced Functional Materials*, vol. 27, no. 43, p. 1702394, 2017, doi: 10.1002/adfm.201702394.
- [24] S. Wang *et al.*, "Scalable Fabrication of Photochemically Reduced Graphene-Based Monolithic Micro-Supercapacitors with Superior Energy and Power Densities," *ACS Nano*, vol. 11, no. 4, pp. 4283–4291, Apr. 2017, doi: 10.1021/acs.nano.7b01390.
- [25] S. Zheng *et al.*, "Ionic liquid pre-intercalated MXene films for ionogel-based flexible micro-supercapacitors with high volumetric energy density," *Journal of Materials Chemistry A*, vol. 7, no. 16, pp. 9478–9485, Apr. 2019, doi: 10.1039/C9TA02190F.
- [26] S. Zheng *et al.*, "All-solid-state flexible planar lithium ion micro-capacitors," *Energy Environ. Sci.*, vol. 11, no. 8, pp. 2001–2009, Aug. 2018, doi: 10.1039/C8EE00855H.
- [27] A. Magrez *et al.*, "Low-temperature, highly efficient growth of carbon nanotubes on functional materials by an oxidative dehydrogenation reaction," *ACS Nano*, vol. 4, no. 7, pp. 3702–3708, 2010, doi: 10.1021/nn100279j.
- [28] M. K. Hota, Q. Jiang, Y. Mashraei, K. N. Salama, and H. N. Alshareef, "Fractal Electrochemical Microsupercapacitors," *Advanced Electronic Materials*, vol. 3, no. 10, Oct. 2017, doi: 10.1002/aelm.201700185.
- [29] C. Y. Lee, H. M. Tsai, H. J. Chuang, S. Y. Li, P. Lin, and T. Y. Tseng, "Characteristics and Electrochemical Performance of Supercapacitors with Manganese Oxide-Carbon Nanotube



- Nanocomposite Electrodes," *Journal of The Electrochemical Society*, vol. 152, no. 4, p. A716, 2005, doi: 10.1149/1.1870793.
- [30] H. Zhang, G. Cao, Z. Wang, Y. Yang, Z. Shi, and Z. Gu, "Influence of Hydrogen Pretreatment Condition on the Morphology of Fe/Al<sub>2</sub>O<sub>3</sub> Catalyst Film and Growth of Millimeter-Long Carbon Nanotube Array," *J. Phys. Chem. C*, vol. 112, no. 12, pp. 4524–4530, Mar. 2008, doi: 10.1021/jp710338d.
- [31] O. Pitkänen *et al.*, "On-chip integrated vertically aligned carbon nanotube based super- and pseudocapacitors," *Scientific Reports*, vol. 7, no. 1, pp. 1–7, 2017, doi: 10.1038/s41598-017-16604-x.
- [32] S. Esconjauregui *et al.*, "Measurement of area density of vertically aligned carbon nanotube forests by the weight-gain method," *Journal of Applied Physics*, vol. 113, no. 14, p. 144309, Apr. 2013, doi: 10.1063/1.4799417.
- [33] Y. Zhou *et al.*, "Ultrahigh-Areal-Capacitance Flexible Supercapacitor Electrodes Enabled by Conformal P3MT on Horizontally Aligned Carbon-Nanotube Arrays," *Advanced Materials*, vol. 31, no. 30, pp. 1–8, 2019, doi: 10.1002/adma.201901916.
- [34] K.-H. Choi, J. Yoo, C. K. Lee, and S.-Y. Lee, "All-inkjet-printed, solid-state flexible supercapacitors on paper," *Energy Environ. Sci.*, vol. 9, no. 9, pp. 2812–2821, Aug. 2016, doi: 10.1039/C6EE00966B.
- [35] E. Raymundo-Piñero, V. Khomenko, E. Frackowiak, and F. Béguin, "Performance of Manganese Oxide/CNTs Composites as Electrode Materials for Electrochemical Capacitors," *Journal of The Electrochemical Society*, vol. 152, no. 1, p. A229, Dec. 2004, doi: 10.1149/1.1834913.
- [36] Y. Liu *et al.*, "A New High-Current Electrochemical Capacitor Using MnO<sub>2</sub>-Coated Vapor-Grown Carbon Fibers," *Crystals*, vol. 12, no. 10, Art. no. 10, Oct. 2022, doi: 10.3390/cryst12101444.
- [37] Y. J. Kang, H. Chung, and W. Kim, "1.8-V flexible supercapacitors with asymmetric configuration based on manganese oxide, carbon nanotubes, and a gel electrolyte," *Synthetic Metals*, vol. 166, pp. 40–44, Feb. 2013, doi: 10.1016/j.synthmet.2013.01.013.
- [38] J.-H. Jeong, J. W. Park, D. W. Lee, R. H. Baughman, and S. J. Kim, "Electrodeposition of  $\alpha$ -MnO<sub>2</sub>/ $\gamma$ -MnO<sub>2</sub> on Carbon Nanotube for Yarn Supercapacitor," *Scientific Reports*, vol. 9, no. 1, p. 11271, Aug. 2019, doi: 10.1038/s41598-019-47744-x.